

## ARTICLE

# Perturbed CD8<sup>+</sup> T cell immunity across universal influenza epitopes in the elderly

Thi H. O. Nguyen<sup>1</sup> | Sneha Sant<sup>1</sup> | Nicola L. Bird<sup>1</sup> | Emma J. Grant<sup>1,2,3</sup> |  
E. Bridie Clemens<sup>1</sup> | Marios Koutsakos<sup>1</sup> | Sophie A. Valkenburg<sup>1,5</sup> | Stephanie Gras<sup>3,4</sup> |  
Martha Lappas<sup>6,7</sup> | Anthony Jaworowski<sup>8,9</sup> | Jane Crowe<sup>10</sup> | Liyen Loh<sup>1</sup> |  
Katherine Kedzierska<sup>1</sup>

<sup>1</sup>Department of Microbiology and Immunology, The University of Melbourne, Peter Doherty Institute for Infection and Immunity, Melbourne, Victoria, Australia

<sup>2</sup>Division of Infection and Immunity, Cardiff University School of Medicine, Heath Park, Cardiff, United Kingdom

<sup>3</sup>Infection and Immunity Program and Department of Biochemistry and Molecular Biology, Biomedicine Discovery Institute, Monash University, Clayton, Victoria, Australia

<sup>4</sup>Australian Research Council Centre of Excellence for Advanced Molecular Imaging, Monash University, Clayton, Victoria, Australia

<sup>5</sup>Pasteur School of Public Health, The University of Hong Kong, Hong Kong SAR, Republic of China

<sup>6</sup>Obstetrics, Nutrition and Endocrinology Group, Department of Obstetrics and Gynaecology, The University of Melbourne, Victoria, Australia

<sup>7</sup>Mercy Perinatal Research Centre, Mercy Hospital for Women, Heidelberg, Victoria, Australia

<sup>8</sup>Department of Infectious Diseases, Alfred Hospital and Monash University, Melbourne, Victoria, Australia

<sup>9</sup>Centre for Biomedical Research, Burnet Institute, Melbourne, Victoria, Australia

<sup>10</sup>Deerpene Surgery, Deerpene, Victoria, Australia

## Correspondence

Liyen Loh, Department of Microbiology and Immunology, The University of Melbourne, Peter Doherty Institute for Infection and Immunity, Royal Parade, Parkville, VIC 3010, Australia.

E-mail: loh@unimelb.edu.au

Katherine Kedzierska, Department of Microbiology and Immunology, The University of Melbourne, Peter Doherty Institute for Infection and Immunity, Royal Parade, Parkville, VIC 3010, Australia.

E-mail: kkedz@unimelb.edu.au;

Twitter: <http://www.twitter.com/kedzierskalab>

## Abstract

Influenza epidemics lead to severe illness, life-threatening complications, and deaths, especially in the elderly. As CD8<sup>+</sup> T cells are associated with rapid recovery from influenza, we investigated the effects of aging on antigen-specific CD8<sup>+</sup> T cells across the universal influenza epitopes in humans. We show that aging is characterized by altered frequencies in T cell subsets, with naive T cells being partially replaced by activated effector/memory populations. Although we observed no striking differences in TCR signaling capacity, T cells in the elderly had increased expression of transcription factors Eomes and T-bet, and such changes were most apparent in CD8<sup>+</sup> T cells. Strikingly, the numbers of antigen-specific CD8<sup>+</sup> T cells across universal influenza epitopes were reduced in the elderly, although their effector/memory phenotypes remained stable. To understand whether diminished numbers of influenza-specific CD8<sup>+</sup> T cells in the elderly resulted from alteration in TCR clonotypes, we dissected the TCR $\alpha\beta$  repertoire specific for the prominent HLA-A\*02:01-restricted-M1<sub>58-66</sub> (A2/M1<sub>58</sub>) influenza epitope. We provide the first ex vivo data on paired antigen-specific TCR $\alpha\beta$  clonotypes in the elderly, showing that influenza-specific A2/M1<sub>58</sub><sup>+</sup> TCR $\alpha\beta$  repertoires in the elderly adults varied from those in younger adults, with the main features being a reduction in the frequency of the public TRAV27-TRBV19 TCR $\alpha\beta$  clonotype, increased proportion of private TCR $\alpha\beta$  signatures, broader use of TRAV and TRBV gene segments, and large clonal expansion of private TCR $\alpha\beta$  clonotypes with longer CDR3 loops. Our

Abbreviations: A2/M1<sub>58</sub>, HLA-A\*02:01-restricted M1<sub>58-66</sub> GILGFVFTL epitope; AD, young adult donor; APC, allophycocyanin; ARCBS, Australian Red Cross Blood Service; B8/NP<sub>225</sub>, HLA-B\*08:01-NP<sub>225-233</sub>; B27/NP<sub>383</sub>, HLA-B\*27:05-NP<sub>383-391</sub>; B57/NP<sub>199</sub>, HLA-B\*57:01-NP<sub>199-207</sub>; CB, cord blood; dn, day *n*; ED, elderly adult donor; Eomes, Eomesoderm; HCMV, human CMV; HCV, hepatitis C virus; M1, matrix protein 1; MFI, mean fluorescent intensity; MHC-I, MHC class I; NP, nucleoprotein; SA, streptavidin; TAME, tetramer-associated magnetic enrichment; TRAJ/BJ, TCR $\alpha/\beta$  joining; TRAV/BV, TCR $\alpha/\beta$  variable

study supports the development of T cell-targeted influenza vaccines that would boost the T cell compartment during life and maintain the numbers and optimal TCR $\alpha\beta$  signatures in the elderly.

#### KEYWORDS

TCR repertoire, transcription factors, ZAP-70, CD8<sup>+</sup> T cells, aging

## 1 | INTRODUCTION

Circulating influenza viruses are an enormous global health burden, with an annual estimate of 3–5 million cases of severe illness and 250,000–500,000 deaths worldwide (<http://www.who.int/mediacentre/factsheets/fs211/en/>; World Health Organization, updated November 2016), despite annual updates of the influenza vaccine components. Most people experience mild to moderate influenza illness only once or twice in their lifetime,<sup>1</sup> with symptoms ranging from fever, cough, sore throat, body aches, and fatigue. However, the risk of severe influenza illness, which often requires hospitalization and can result in death, is more pronounced in the elderly, with increased occurrence, higher hospitalization rates, and increased morbidity and mortality compared with younger adults.<sup>2–4</sup> This is exemplified by the data obtained from 17 Australian major hospitals during the 2015 April–October influenza season, with the elderly ( $\geq 65$  yr) accounting for 46% of all hospitalized influenza-infected patients out of 2070 laboratory-confirmed cases.<sup>3</sup> Elderly individuals, particularly men, also preferentially succumbed to severe avian H7N9 influenza disease.<sup>2,5,6</sup> Such increased susceptibility and morbidity/mortality of influenza infections in the elderly might be partially a result of coexisting comorbidities (i.e. diabetes, chronic respiratory, cardiac, or renal disease) in this age group. Concomitantly, aging is also associated with decreased or impaired function of the immune system, named as immunosenescence.<sup>7</sup>

As established T cell immunity directed at conserved viral regions can provide protection against influenza viruses and lead to more rapid host recovery,<sup>2,8–10</sup> prolonged influenza disease in the elderly indicates an impairment within the T cell compartment. Indeed, aging can have multifactorial effects on T cell immunity, arising from decreased thymic export of naive precursors, due to thymic involution,<sup>11,12</sup> perturbed recruitment of naive CD8<sup>+</sup> T cell precursors,<sup>13,14</sup> replicative senescence of memory T cells,<sup>15–18</sup> and decreased cytolytic function, as measured by granzyme B production.<sup>19,20</sup> Aging can also affect TCR composition of naive and immune T cells in mice, with large antigen-independent clonal expansion.<sup>21</sup> Naive T cell attrition has also been inferred from observed reductions in the diversity of antigen-specific TCR repertoires in aged mice<sup>22–24</sup> and humans.<sup>25</sup>

Our group recently established that human pre-existing memory CD8<sup>+</sup> T cells can recognize universally conserved epitopes derived from the internal influenza proteins, matrix protein (M1) and NP, which were present across different influenza A virus strains circulating during the past century,<sup>26</sup> including the novel avian A/H7N9 influenza virus.<sup>6,27,28</sup> Indeed, these universal influenza CD8<sup>+</sup> T cell epitopes are restricted to common HLA class I types, HLA-A\*02:01, HLA-A\*03:01, HLA-B\*08:01, HLA-B\*18:01, HLA-B\*27:05, and HLA-B\*57:01,<sup>26</sup>

which are prevalent across many different ethnicities. Although recently, van de Sandt et al.<sup>29</sup> demonstrated elegantly the persistence and longevity of influenza-specific CD8<sup>+</sup> T cells over 13 years (1999–2012), in 9 healthy donors, aged between 18 and 64, it is still unclear whether the numbers of influenza-specific CD8<sup>+</sup> T cells, especially those directed at the universal influenza epitopes, persist or decline in individuals older than 65 yr of age. To understand T cell responses attributed to the declining immunity, we dissected influenza-specific CD8<sup>+</sup> T cell responses and TCR $\alpha\beta$  clonal composition in EDs compared with younger or middle-aged adults. We analyzed the effects of aging on both the total (not antigen-specific) CD8<sup>+</sup> and CD4<sup>+</sup> T cell compartments, their frequencies, effector/memory phenotypes, and expression of transcription factors, as well as antigen-specific CD8<sup>+</sup> T cell immunity directed at universal influenza epitopes, together with their phenotypes and TCR $\alpha\beta$  repertoires. We found that whereas bulk T cell compartments are associated with increased frequencies of effector/memory T cells and altered transcription factor levels, the numbers of influenza-specific CD8<sup>+</sup> T cells are lower in elderly individuals and display large, noncanonical clonal expansions and reduced use of the preferred TCR $\alpha\beta$  signatures, such as TRBV19, TRAV27, and the public TRBV19–TRAV27 clonotype. Our study indicates the need for new vaccination strategies to preserve the numbers and optimal TCR $\alpha\beta$  features of influenza-specific CD8<sup>+</sup> T cell immunity in elderly individuals.

## 2 | MATERIALS AND METHODS

### 2.1 | Human blood samples

Human experimental work was conducted according to Declaration of Helsinki principles and approved by the Human Ethics Committee (Ethics ID #0931311.5 and #1443389.3; University of Melbourne, Parkville, VIC, Australia). Peripheral blood was obtained from healthy, younger adults (ADs), recruited at the University of Melbourne (aged 25–58 yr), or EDs, recruited at Deerpene Medical Clinic (Deerpene, VIC, Australia; aged 60+ yr). The vaccination status of the donors, when known, is listed in Table 1. The Immunise Australia Program (Canberra ACT, Australia) provides the seasonal influenza immunization around April each year. Influenza immunization is freely available from general practice and other immunization providers for people who are at high risk of influenza and its complications, including people aged 65 and over and pregnant women.

Buffy packs from healthy donors (aged 22–70 yr) were obtained from the ARCBS (West Melbourne, VIC, Australia). Umbilical CB was obtained from the Mercy Hospital for Women (Heidelberg, Australia).

**TABLE 1** Cohort demographics of all donors used in the study

Donor code	Age	HLA-A or -A <sup>a</sup>	HLA-B or -B <sup>a</sup>	Figure	Vaccination status <sup>b</sup>	Year of vaccination (if known)
Cord blood						
CB1	0			1A and B	NA	–
CB2	0			1B	NA	–
CB3	0			1B	NA	–
CB4	0			1B	NA	–
CB5	0			1B	NA	–
CB6	0	02:01, 31:01	27:05, 38:01	1B	NA	–
CB7	0			1A and B	NA	–
CB8	0			1B	NA	–
Adult healthy volunteers						
AD2	27	02:01, 11:01	35:01, 39:01	3B, 5B–D, and 6A	Yes	2016
AD3	41	01:01, 68:01	35:03, 37:01	1A and B	Yes	2017
AD4	31	02:01, 11:01	40:01, 44:02	3B and 5C, upper and lower	Yes	2014
AD5	31	01:01, 26:01	08:01, 44:03	1A and B	Yes	2014
AD6	40	01:01, 03:01	08:01, 15:01	1A and B	Yes	
AD11	25	02:01, 11:01	35:01, 39:01	5B–D and 6A	Yes	2014
AD15	31	01:01, 11:01	35:01, 52:01	1A and B	Yes	2014, 2015
AD16	46	02:01, 11:01	35:03, 44:02	3B	Yes	
AD17	29	32:01	07:02, 44:02	1C and D	Yes	2010
AD18	42	02:01, 03:02	18:01, 35:08	3B	Yes	2015
AD19	28	01:01	08:01	3A and B	Yes	2014
AD21 <sup>c</sup>	29	26:01, 33:03	40:02, 52:01	1B	Yes	2014, 2015, 2016
AD21 <sup>c</sup>	31	26:01, 33:03	40:02, 52:01	1B and 2B and C	Yes	2014, 2015, 2016
AD25 <sup>c</sup>	26			1A and B	Yes	2015, 2016
AD25 <sup>c</sup>	29			1B and 2B and C	Yes	2015, 2016
AD26	25	11:01, 26:01	14:01, 27:05	Fig. 1B and 2B and C	Yes	2015, 2016
AD27	29	02:01	15:01, 44:02	1B	Yes, before 2009 pH1N1	2008
AD28	30	02:07, 11:01	15:02, 57:01	1B and 2B and C	Yes	2014, 2015, 2016, 2017
AD40	29	03:01, 33:03	35:01, 44:03	1B	Yes	2014, 2015, 2016
AD51	31	02:01, 33:03	07:02, 27:02	3B	Yes	2015, 2016
AD52	47	02:01, 03:01	07:02, 55:02	1A and B	Yes	2015
AD69	58	2, 3	14, 27	1B and 3B	Yes	2011, 2012, 2013, 2014, 2015, 2016, 2017
AD101	30	02:01, 34:01	13:01, 40:01	5C and D and 6A	ND	–
AD102	45	02:01, 34:01	13:01, 56:01	5C and D and 6A	ND	–
Adult buffy packs						
AD13	50	02:01, 68:01	27:05, 15:18	3B	ND	–
AD23	22	02:01, 68:01	44:02, 51:01	5B–D and 6A	ND	–
AD24	48	01:02, 02:01	08:01, 44:02	4B and C	ND	–
AD30	53	02:01, 30:04	15:03, 57:01	3A and B and 5C, upper and lower	ND	–
AD29	54	03:01, 26:01	07:02, 27:05	3B and 5C, upper and lower	ND	–
AD31	50	02:01, 26:01	07:02, 27:05	3A and B	ND	–
AD34	30	02:01, 03:01	40:01 (60), 56:01	3B and 5C, upper and lower	ND	–
AD36	25	02:01, 03:01	07:02, 40:01	3B and 5C, upper and lower	ND	–
AD48	47	02:01, 29:02	15:01, 35:01	4A–C	ND	–

(Continues)

**TABLE 1** (Continued)

Donor code	Age	HLA-A or -A <sup>a</sup>	HLA-B or -B <sup>a</sup>	Figure	Vaccination status <sup>b</sup>	Year of vaccination (if known)
AD60	54	02:01, 03:01	35:01, 57:01	3B and 5C, upper and lower	ND	–
AD71	56	02:01	07:02, 57:01	3A and B	ND	–
AD73	45			1D	ND	–
AD76	31	02:01, 02:05	44:02, 50:01	3B and 5C, upper and lower	ND	–
AD78	50			1D	ND	–
AD86	51	02:01	07:02, 39:01	3B and 5C, upper and lower	ND	–
AD87	58	02:01, 32:01	40:01, 44:02	3B and 5C, upper and lower	ND	–
AD88	22	02:01, 11:01	15:02, 54:01	3B and 5C, upper and lower	ND	–
AD94	25	02:01, 24:02	27:05, 35:01	3B and 5C, upper and lower	ND	–
AD95	43	02:01	07:02, 44:02	3B and 5C, upper and lower	ND	–
AD97	36	02:01, 02:05	07:02, 44:01	3B and 5C, upper and lower	ND	–
AD100	45	02:01	07:02, 44:02	3B and 5C, upper and lower	ND	–
AD103	<60	2	18	3B	ND	–
AD104	<60	02:01, 2501	07:02, 18:01	3B	ND	–
AD105	<60	2, 24	7, 40	3B	ND	–
Elderly adults						
ED1	87	02:01, 31:01	40:01, 44:02	3B	Yes	2009, p2009, 2010, 2011, 2012, 2013, 2014, 2015
ED3	73	02:01	07:02, 44:02	2B and C, 3B, and 5C, upper and lower	Yes	2007, 2009, p2009, 2010, 2011, 2012, 2013, 2014
ED4	81	01:01, 24:02	08:01, 57:01	2B and C and 3A and B	Yes	2007, 2009, 2010, 2011, 2013, 2014, 2015
ED5	84	02:01, 11:01	13:02, 44:02	3B	ND	
ED6	75	01:01, 31:01	07:02, 44:03	2B and C	ND	
ED7	81			1D	ND	
ED8	78			2B and C	ND	
ED9	76	02:01, 03:01	37:01, 44:02	1A and B, 5A–E, and 6A–C	ND	
ED11	78			2B and C	ND	
ED12	65	02:01, 24:02	27:05, 40:01	3B	ND	
ED15	66	01:01, 02:01	08:01, 27:05	3B	ND	
ED16	72	01:01, 29:02	08:01, 44:03	1B and 2B and C	ND	
ED17	81	11:01, 23:01	27:05, 44:03	2B and C and 3A and B	ND	
ED18	66	02:01	15:01, 44:02	4B and C, 5A–E, and 6A–C	ND	
ED19	83	01:01, 02:01	08:01, 13:02	2B and C and 3A and B	Yes	2009, p2009, 2010, 2011, 2012, 2013
ED20	82	02:01, 03:01	27:05, 44:02	3B	Yes	2009, p2009, 2010, 2011, 2012, 2013
ED21	79	01:01	37:01, 57:01	1B and 2B and C	Yes	2008, 2009, p2009, 2010, 2011, 2012, 2013
ED22	73	03:01, 33:03	15:01, 58:01	1B and 2B and C	Yes	2008, 2009, p2009, 2010, 2011, 2012, 2013
ED23	74	01:01, 68:01	08:01, 44:02	1B and 2B and C	Yes	2007, 2008, 2009, p2009, 2010, 2011, 2012, 2013
ED24	77	02:01	35:01, 40:01	2B and C, 3B, 4A and B, and 5C, upper and lower	Yes	2008, 2009, p2009, 2010, 2011, 2012, 2013
ED25	76	02:01, 03:01	07:02, 39:06	2B and C, 3B, 4A–C, and 5C, upper and lower	Yes	2009, 2010, 2011, 2012, 2013
ED26	77	02:05, 26:01	38:01, 49:01	1B and 2B and C	Yes	2007, 2009, p2009, 2010, 2011, 2012, 2013
ED27	88	03:01, 33:01	14:02, 15:01	1B and 2B and C	Yes	2007, 2009, 2010, 2011, 2012, 2013

(Continues)

**TABLE 1** (Continued)

Donor code	Age	HLA-A or -A <sup>a</sup>	HLA-B or -B <sup>a</sup>	Figure	Vaccination status <sup>b</sup>	Year of vaccination (if known)
ED28	80	02:01, 11:01	<b>27:05</b> , 55:01	2B and C and 3B	Yes	2005, 2007, 2009, 2010, 2011, 2012, 2013, p2009
ED31	61	<b>02:01</b> , 03:01	07:02, 50:01	3A and B, 5A–E, and 6A–C	Yes	
ED33	82	03:01, 30:02	18:01, 35:01	1D	Yes	2015
ED36	66	01:01, 03:01	08:01, 40:02	1A and B	Yes	2013, 2015
ED37	82	<b>02:01</b> , 11:01	<b>08:01</b> , 41:02	3B	Yes	2007, 2009, p2009, 2010, 2012, 2013, 2015
ED38	68	<b>02:01</b>	15:01	1D, 2B and C, 3B, and 5, upper and lower	Yes	2012, 2013, 2014, 2015
ED39	84	01:01	<b>08:01</b> , 57:01	3B and 5, upper and lower	Yes	2010, 2011, 2012, 2013, 2014, 2015
Elderly adult buffy packs						
ED102 <sup>d</sup>	70			1C and D	ND	–
ED103 <sup>d</sup>	68			1D	ND	–
ED104	62			2D	ND	–
ED41 <sup>d</sup>	69	<b>02:01</b> , 32:01	07:02, 44:03	3B and 5C, upper and lower	ND	–
ED42 <sup>d</sup>	62	<b>02:01</b>	07:02, 44:02	3B and 5C, upper and lower	ND	–
ED43 <sup>d</sup>	67	01:01, <b>02:01</b>	13:02, 44:32	3B and 5C, upper and lower	ND	–

HLA boldface indicates donors and their HLA used for TAME (Fig. 3). NA, Not applicable; ND, not determined.

<sup>a</sup>Molecular resolution of HLA class I antigens (4-digit) is shown where available.

<sup>b</sup>Vaccinated, post-2009 (p2009) pandemic H1N1 (pH1N1).

<sup>c</sup>Of note, AD21 and AD25 were bled twice.

<sup>d</sup>EDs obtained from buffy packs; therefore, vaccination status ND.

**TABLE 2** Highly conserved “universal” influenza epitopes used in this study

HLA restriction	Peptide	Sequence	Epitope acronym
HLA-A*02:01	M1 <sub>58–66</sub>	GILGFVFTL	A2/M1 <sub>58</sub>
HLA-B*08:01	NP <sub>225–233</sub>	ILKGKFQTA	B8/NP <sub>225</sub>
HLA-B*27:05	NP <sub>383–391</sub>	SRYWAIKTR	B27/NP <sub>383</sub>
HLA-B*57:01	NP <sub>199–207</sub>	RGINDRNFW	B57/NP <sub>199</sub>

All donors provided informed written consent. PBMCs were isolated by Ficoll-Paque (GE Healthcare, Uppsala, Sweden) density gradient centrifugation and cryopreserved at  $-196^{\circ}\text{C}$  until required. HLA class I molecular typing was performed as previously described<sup>30</sup> by the Victorian Transplantation and Immunogenetics Service (ARCBS).

## 2.2 | Peptides and tetramers

Influenza A peptides derived from M1 and NP proteins (Table 2) were purchased from GenScript (Piscataway, NJ, USA). Monomers were generated in house by refolding each peptide with its restricted HLA (Table 2)  $\alpha$ -heavy chain–BirA and  $\beta$ 2-microglobulin<sup>31</sup> before 8:1 M conjugation with PE-SA or APC-SA (BD Biosciences, San Jose, CA, USA) to form tetramers.

## 2.3 | Flow cytometry

PBMCs were thawed and cell-surface stained in MACS buffer (PBS containing 0.5% BSA/2 mM EDTA) with human anti-CD3 PE-CF594

(#562280; BD Biosciences), anti-CD4 BV650 (#563875; BD Biosciences), anti-CD8 PerCP-Cy5.5 (#565310; BD Biosciences) or anti-CD8 BV605 (#301039; BioLegend, San Diego, CA, USA), anti-CD14 APC-H7 (#560180; BD Biosciences) or anti-CD14 BV570 (#301831; BioLegend), anti-CD19 APC-H7 (#560177; BD Biosciences) or anti-CD19 BV570 (#302235; BioLegend), anti-CD45RA-FITC (#555488; BD Biosciences) or anti-CD45RA APC-H7 (#560674; BD Biosciences), anti-CD27 AF700 (#56027942; eBioscience, San Diego, CA, USA) or anti-CD27 BV711 (#563167; BD Biosciences), and LIVE/DEAD Fixable Near-IR (Thermo Fisher Scientific, Waltham, MA, USA) before fixation with 1% paraformaldehyde. For transcription factor staining, cells were fixed and intracellularly stained with anti-Eomes PE (3-4877-42; eBioscience) and anti-T-bet PE-Cy7 (32-5825-82; eBioscience) using the forkhead box P3 transcription factor staining kit (#00-5523-00; eBioscience). Cells were resuspended in MACS buffer and then acquired on an LSRFortessa II (BD Biosciences) and analyzed by FlowJo software (Treestar, Ashland, OR, USA).

## 2.4 | Flow cytometry-based assay for ZAP-70 phosphorylation

Kinetics of TCR stimulation via phosphorylation of ZAP-70 was measured using the BD Phosflow Whole Blood Starter Kit (BD Biosciences). Firstly, 2 whole blood was incubated with anti-CD3 antibody (OKT3 clone; Walter and Eliza Hall Institute of Medical Research, Parkville, VIC, Australia) for 10 min on ice, washed, and then incubated with goat anti-mouse F(ab')<sub>2</sub> for 5 min on ice. TCR signaling was

initiated by incubating the samples in a 37°C water bath before adding Lyse/Fix solution to each time-point tube at 0, 30, 60, 90, 120, and 150 s and 4 and 7 min to stop the reaction. Samples were then incubated with anti-ZAP-70(Y319)/Syk(Y352)-PE (#557881; BD Biosciences) and cell-surface mAb in Perm/Wash buffer on ice, as previously described in Lichtfuss et al.<sup>32</sup> Cells were acquired by flow cytometry.

## 2.5 | PMA and ionomycin stimulation

Adult and elderly PBMCs ( $1 \times 10^6$ ) were stimulated *ex vivo* with PMA (10 ng/ml) and ionomycin (1  $\mu$ M) for 6 h in the presence of protein transport inhibitors Brefeldin A (#555029; BD Biosciences) and Monensin (#554724; BD Biosciences). Samples were subsequently stained with LIVE/DEAD discrimination marker and cell surface mAb, anti-CD3, anti-CD4, and anti-CD8, as above. Cells were then fixed with BD Cytofix/Cytoperm kit (#554722; BD Biosciences) before intracellular staining with anti-IFN- $\gamma$  (#560371; BD Biosciences) and anti-TNF (#557647; BD Biosciences) and samples acquired by flow cytometry, as described above.

## 2.6 | TAME of influenza-specific CD8<sup>+</sup> T cells

Cryopreserved PBMCs ( $4\text{--}35 \times 10^6$ ) were thawed and incubated with anti-human FcR block (Miltenyi Biotec, Bergisch Gladbach, Germany) for 15 min on ice. Cells were then stained with PE- and/or APC-SA-conjugated tetramer for 1 h at room temperature, washed once, and then incubated with anti-PE and/or anti-APC MicroBeads (Miltenyi Biotec) before passing through an LS column (Miltenyi Biotec) to enrich for tetramer<sup>+</sup> cells, as previously described.<sup>30,33–35</sup> Cells were then cell-surface stained and either fixed with 1% paraformaldehyde for acquisition or resuspended in MACS buffer for single-cell sorting.

## 2.7 | T cell proliferation assay

HLA-A2<sup>+</sup> responder PBMCs ( $\sim 1 \times 10^7$ ) were preincubated with cell-trace violet (Violet Proliferation Dye 450, BD Horizon; BD Biosciences) before generating A2/M1<sub>58</sub>-specific CD8<sup>+</sup> T cell lines, as previously described.<sup>26,36</sup> In brief, one-third of unlabeled PBMCs was pulsed with 10  $\mu$ M A2/M1<sub>58–66</sub> peptide for 90 min at 37°C, washed twice, and then incubated with the remaining two-thirds of cell trace violet-labeled autologous PBMCs for 10 d (37°C, 5% CO<sub>2</sub>) in complete RF10 medium containing 10% heat-inactivated FCS, 2 mM L-glutamine, 1 mM MEM sodium pyruvate, 100  $\mu$ M MEM nonessential amino acids, 5 mM HEPES buffer solution, 55  $\mu$ M 2-ME, and 100 U/ml penicillin per 100  $\mu$ g/ml streptomycin in RPMI-1640 media, plus 10 U/ml recombinant IL-2 (Roche Diagnostics, Mannheim, Germany). Media reagents were from Gibco (Thermo Fisher Scientific, Scoresby, VIC, Australia). Cells were assessed on d0, 3, or 4, 5, 6, 7, and 10 by tetramer staining and cell-surface mAb staining, followed by flow cytometry.

## 2.8 | Single-cell RT-PCR and sequencing

PBMCs were stained with tetramer for 1 h at room temperature, washed twice, and then cell-surface stained with mAb. Live CD3<sup>+</sup>CD8<sup>+</sup>tetramer<sup>+</sup>CD19<sup>−</sup>/CD14<sup>−</sup> cells were individually sorted into 96-well twin.tec PCR plates (Eppendorf, Hamburg, Germany) using a BD FACSARIA III (BD Biosciences). Analysis of paired CDR3 $\alpha$  and CDR3 $\beta$  regions was performed by multiplex-nested RT-PCR before sequencing of TCR $\alpha$  and TCR $\beta$  products, essentially as described.<sup>34,35,37,38</sup> Sequences were analyzed according to the IMGT/V-QUEST web-based tool (IMGT, The International ImmunoGeneTics Information System, Montpellier, Cedex, France).<sup>39,40</sup> Circos plots were generated using the Circos software package.<sup>41</sup>

## 2.9 | Statistical analysis

Statistical analysis was carried out using GraphPad Prism software (GraphPad Software, San Diego, CA, USA). Spearman rank analyses were used to derive age-based correlations. Mann-Whitney and Student's *t* test were used where appropriate for comparison between two groups as indicated. Statistical significance is described in figure legends and *r* values stated where relevant.

# 3 | RESULTS

## 3.1 | Distinct age-related profiles within the CD8<sup>+</sup> and CD4<sup>+</sup> T cell compartments

CD8<sup>+</sup> and CD4<sup>+</sup> T cell compartments change throughout a human lifespan. At birth, T cells are predominantly immunologically naive and thereafter, gain the effector/effector memory phenotype with age, consequent to encounters with foreign pathogens. We used two surface phenotypic markers—CD45RA and CD27—to delineate naive (CD45RA<sup>+</sup>CD27<sup>+</sup>), effector/memory (CD45RA<sup>−</sup>CD27<sup>+/−</sup>), and terminally differentiated effector (CD45RA<sup>+</sup>CD27<sup>−</sup>) T cell subsets<sup>33,42</sup> in CB of younger and elderly adults (Fig. 1A), across different ages (a range of 0–88 yr; Table 1). At birth, both CD8<sup>+</sup> and CD4<sup>+</sup> T cells were predominantly of a naive-like CD45RA<sup>+</sup>CD27<sup>+</sup> phenotype ( $\sim 80\%$ ,  $n = 7$ ). Expectedly, the naive CD8<sup>+</sup> and CD4<sup>+</sup> T cell compartments significantly declined with age ( $P < 0.0001$ ;  $r = -0.8232$  and  $-0.7071$ , respectively) to a mean ( $\pm$ SD) of  $44.6 \pm 19.9\%$  in adults ( $n = 16$ ) and  $22.8 \pm 14.0\%$  in the elderly ( $n = 15$ ) for CD8<sup>+</sup> T cells and to  $41.3 \pm 18.1\%$  in younger adults and  $28.2 \pm 14.0\%$  in elderly adults for CD4<sup>+</sup> T cells (Fig. 1Bi). On the other side of the spectrum, terminally differentiated CD45RA<sup>+</sup>CD27<sup>−</sup> CD8<sup>+</sup> T cells<sup>43</sup> significantly increased with age, from  $3.8 \pm 4.1\%$  in CB to  $16.5 \pm 13.0\%$  in younger adults and  $33.3 \pm 12.9\%$  in elderly adults (Fig. 1Bii). Whereas the terminally differentiated CD45RA<sup>+</sup>CD27<sup>−</sup> effector CD8<sup>+</sup> T cell subset was prominent in younger adults and elderly adults, CD45RA<sup>+</sup>CD27<sup>−</sup> CD4<sup>+</sup> T cells were found only at minimal frequencies ( $<3\%$ ) across the human lifespan. Furthermore, the frequency of the activated effector/memory populations lacking CD45RA expression and either CD27<sup>+</sup> (Fig. 1Biii) or



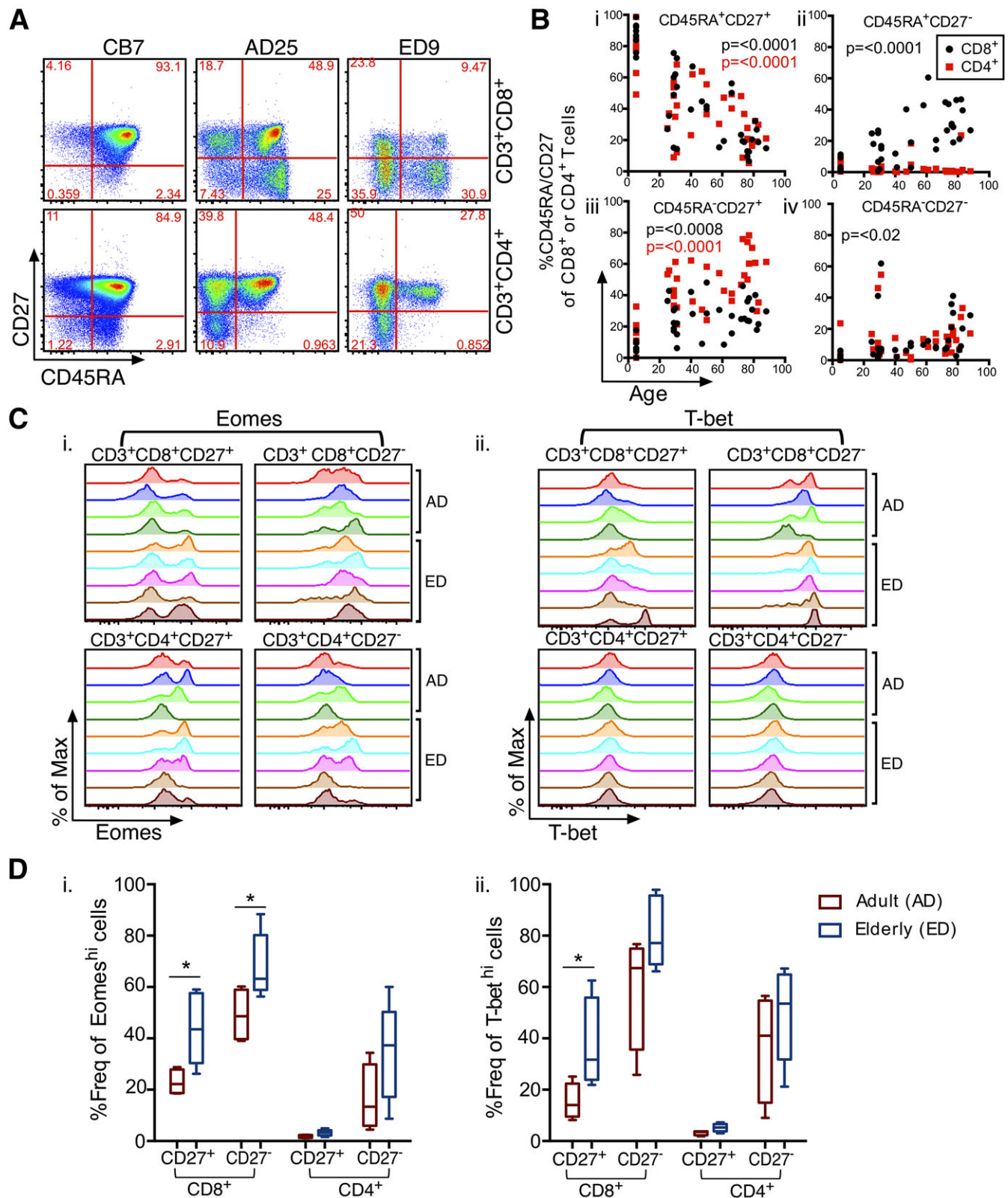


**FIGURE 1** Changes in CD8<sup>+</sup> and CD4<sup>+</sup> T cell compartments with aging. CD8<sup>+</sup> and CD4<sup>+</sup> T cell frequencies and phenotypes were compared among human CB, AD, and ED. (A) Representative FACS plots show 4 subsets of CD8<sup>+</sup> and CD4<sup>+</sup> T cell differentiation in a CB, AD, and ED, based on CD45RA vs. CD27 expression. (B) Frequency of (i) CD45RA<sup>+</sup>CD27<sup>+</sup>, (ii) CD45RA<sup>+</sup>CD27<sup>-</sup>, (iii) CD45RA<sup>-</sup>CD27<sup>+</sup>, and (iv) CD45RA<sup>-</sup>CD27<sup>-</sup> subsets plotted against age for CD8<sup>+</sup> (black circles) and CD4<sup>+</sup> T cells (red squares). P-values in black and red are shown for CD8<sup>+</sup> and CD4<sup>+</sup> T cells, respectively (Spearman rank correlation). (C) Histograms of (i) Eomes and (ii) T-bet expression on CD8<sup>+</sup> (upper) and CD4<sup>+</sup> T cells (lower) in the presence or absence of CD27 coexpression. (D) Box-and-whisker plots of (i) Eomes<sup>hi</sup> and (ii) T-bet<sup>hi</sup> populations in CD27<sup>+</sup> and CD27<sup>-</sup> subpopulations of CD8<sup>+</sup> and CD4<sup>+</sup> T cells in AD (red, *n* = 4) vs. ED (blue, *n* = 5) donors. Rectangles represent the second and third quartiles separated by the median horizontal line. Lower and upper quartiles are shown as vertical lines on either side of the rectangle (\**P* < 0.05, Mann-Whitney)

CD27<sup>-</sup> (Fig. 1Biv) significantly increased with age for both CD8<sup>+</sup> and CD4<sup>+</sup> T cells.

To explore further the transcriptional profiles within activated CD27<sup>-</sup> or resting CD27<sup>+</sup> T cells during aging, we analyzed expression of the key transcription factors for T cell function and differentiation, Eomes, and T-bet.<sup>44</sup> Bimodal distribution of Eomes in CD27<sup>+</sup> T cells demonstrated two populations of “naïve-like” CD27<sup>+</sup>Eomes<sup>lo</sup>T-bet<sup>lo</sup> T cells, also negative for the cytolytic molecules perforin and granzyme (data not shown), and a mixture of effector/memory Eomes<sup>hi</sup>T-bet<sup>hi</sup> T cells heterogeneously expressing CD27 (Fig. 1C). In agreement with previous findings,<sup>42</sup> we observed significantly higher frequencies of Eomes<sup>hi</sup> expression in both CD27<sup>+</sup> ( $P = 0.0317$ ) and CD27<sup>-</sup> ( $P = 0.0317$ ) CD8<sup>+</sup> T cell populations and higher frequencies of T-bet<sup>hi</sup> expression in CD27<sup>+</sup>CD8<sup>+</sup> T cells ( $P = 0.0317$ ) in elderly individuals compared with younger adults (Fig. 1D). Although similar trends were observed in CD4<sup>+</sup> T cells, these were not significant.

Thus, with aging, naïve T cells are replaced with the activated effector/memory T cell subsets, characterized by increasing Eomes/T-bet expression, and such changes are most apparent in the CD8<sup>+</sup> T cell compartment.

### 3.2 | Elderly CD8<sup>+</sup> and CD4<sup>+</sup> T cells retain their TCR signaling capacity

As the composition of T cell compartments and their transcription factor profiles change with age, we next asked whether aging also affects the initial TCR engagement and TCR signaling efficacy. We measured the kinetics of tyrosine phosphorylation of ZAP-70, which plays a critical role in T cell signal transduction after TCR-dependent activation. TCR stimulation was initiated by cross-linking with anti-CD3 antibody, and the kinetic analysis of the peak geometric MFI of ZAP-70 phosphorylation was measured in CD8<sup>+</sup> and CD4<sup>+</sup> T cells after 0, 30, 60, 90, 120, and 150 s and 4 and 7 min of TCR stimulation (Fig. 2A). Evidently, there were no significant differences in ZAP-70 phosphorylation kinetics for either CD8<sup>+</sup> or CD4<sup>+</sup> T cell populations between EDs and ADs, as assessed by phospho-ZAP-70 MFI, measured as fold changes from the baseline (Fig. 2B). ZAP-70 phosphorylation was initiated between 60 and 90 s for both T cell subsets and peaked at 120 s for CD8<sup>+</sup> T cells and 150 s for CD4<sup>+</sup> T cells, albeit the 30 s delay was not significant. As a negative control, non-T cells (CD3<sup>-</sup> lymphocytes), including NK cells, which also show increased phosphorylated ZAP-70/Syk staining when activated, remained inactive during anti-CD3 cross-linking and showed stable expression of ZAP-70 over time (Fig. 2A).

Given that the distribution of T cell subset changes with age, as shown by a decline in naïve-like T cells and an increase in effector/memory T cell subsets (Fig. 1), we further examined TCR signaling capacity within the phenotypically distinct T cell subsets of adults and the elderly. In the CD8<sup>+</sup> T cell compartment, we observed no significant differences in the naïve/effector/memory subsets between younger and elderly adults (Fig. 2C, left). However, the CD45RA<sup>-</sup>CD27<sup>-</sup> effector memory subset within CD4<sup>+</sup> T cells showed significantly higher ZAP-70 MFI fold change at 150 s and 4 min in the EDs (Fig. 2C, right), suggesting that effector memory CD4<sup>+</sup> T cells in

the elderly may have a higher and prolonged signaling capacity compared with younger individuals.

To assess the functional capacity of adult and elderly T cells, we assessed cytokine (IFN- $\gamma$  and TNF) production by PBMCs stimulated *ex vivo* with PMA and ionomycin. No significant differences ( $P > 0.05$ ) in the single or dual cytokine-producing T cells were observed across the CD8<sup>+</sup> and CD4<sup>+</sup> T cell compartments within younger adults ( $n = 7$ ) to elderly adults ( $n = 7$ ; Fig. 2D).

Overall, although aging is associated with altered frequencies in T cell subsets and transcription profiles, no striking differences in TCR signaling or cytokine producing capacity, especially in CD8<sup>+</sup> T cells, were observed.

### 3.3 | Aging is associated with reduced numbers of antigen-specific memory CD8<sup>+</sup> T cells across universal influenza HLAs

Following the broad analysis of total CD8<sup>+</sup> and CD4<sup>+</sup> T cells in the elderly, we subsequently dissected T cells directed at a single epitope level. As influenza virus infections cause significant morbidity and mortality in the elderly, and CD8<sup>+</sup> T cells are associated with rapid recovery,<sup>2,8–10</sup> we investigated whether aging affects the numbers of CD8<sup>+</sup> T cells across the universal influenza HLAs in humans.<sup>26</sup> To enumerate influenza-specific memory CD8<sup>+</sup> T cells in elderly adults compared with younger adults, we used a TAME method, which increases detection of tetramer-positive CD8<sup>+</sup> T cells by up to 100-fold.<sup>30,35,45</sup> Dual enrichment with 2 tetramers was used when donors had  $>1$  of the universal HLAs (Table 1, boldface type). Tetramer-enriched, influenza-specific CD8<sup>+</sup> T cell precursor frequencies were calculated based on the total CD8<sup>+</sup> T cell population, according to Alanio et al.,<sup>45</sup> where  $1 \times 10^{-4}$  represents a frequency of 1 in 10,000 CD8<sup>+</sup> T cells. We assessed enriched memory precursor frequencies for 4 universal HLA/peptide tetramers (A2/M1<sub>58</sub>, B8/NP<sub>225</sub>, B27/NP<sub>383</sub>, and B57/NP<sub>199</sub>; Fig. 3A and Table 2). Our analysis showed significantly reduced numbers of influenza-specific CD8<sup>+</sup> T cells across 2 universal influenza epitopes tested: A2/M1<sub>58</sub> and B27/NP<sub>383</sub> (Fig. 3B). The mean ( $\pm$ SEM) frequency of A2/M1<sub>58</sub><sup>+</sup>CD8<sup>+</sup> T cells was  $2.78 \times 10^{-4} \pm 6.21 \times 10^{-5}$  cells (of total CD8<sup>+</sup> T cells) in younger adults (range:  $1.48 \times 10^{-5}$ – $1.04 \times 10^{-3}$ ) vs.  $8.07 \times 10^{-5} \pm 2.58 \times 10^{-5}$  cells (range:  $2.15 \times 10^{-5}$ – $5.05 \times 10^{-4}$ ) in elderly adults ( $P = 0.0154$ ), whereas for B27/NP<sub>383</sub><sup>+</sup>CD8<sup>+</sup> T cells, there were, on average,  $3.73 \times 10^{-5} \pm 6.88 \times 10^{-6}$  cells in younger adults (range:  $1.62 \times 10^{-5}$ – $5.05 \times 10^{-5}$ ) and  $1.41 \times 10^{-5} \pm 2.67 \times 10^{-6}$  cells (range:  $1.12 \times 10^{-5}$ – $1.94 \times 10^{-5}$ ) in elderly adults ( $P = 0.0481$ ). Of note, as a result of the limited number of donors available for B8/NP<sub>225</sub> and B57/NP<sub>199</sub> TAME experiments, statistical analysis could not be performed, and data points were graphed together (Fig. 3B). Furthermore, phenotypic analysis of A2/M1<sub>58</sub><sup>+</sup>CD8<sup>+</sup> T cells revealed comparable activation/memory phenotypes, as defined by CD45RA and CD27 profiling (Fig. 3C). Furthermore, as we found no difference ( $P = 0.111$ ) in the vaccination rate between our healthy adult volunteers (46%) and EDs (43%), for the donors with known vaccination history, it seems unlikely that the vaccination status of the donors would impact our results.



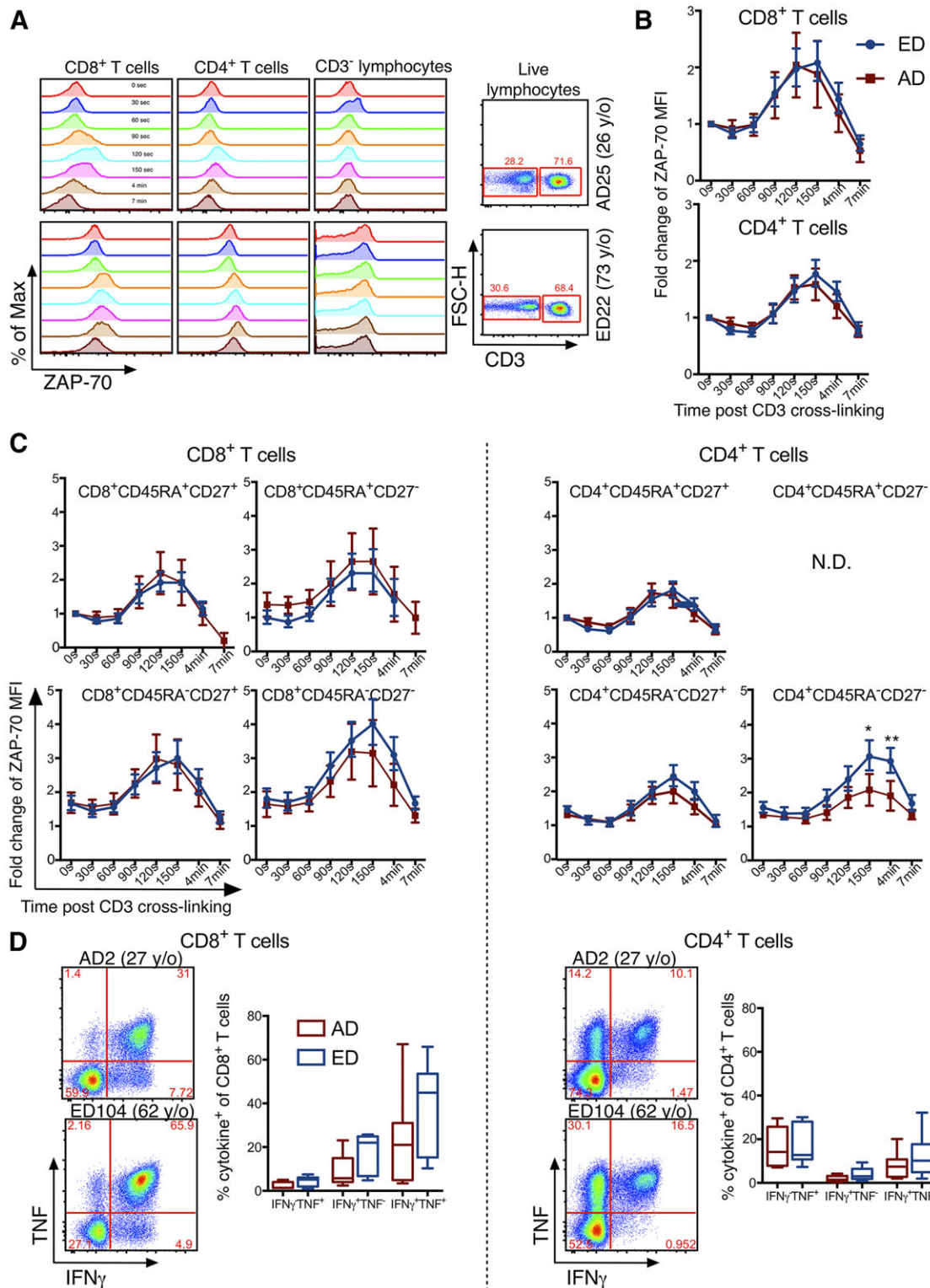


**FIGURE 2** Phosflow measurement of CD3-dependent ZAP-70 in T cell subsets. (A) Representative histograms are shown for ZAP-70 expression in T cell subsets and non-T cells following CD3 cross-linking in an AD and ED at indicated times. (Right) Representative FACS plots of CD3<sup>-</sup> non-T cells and CD3<sup>+</sup> T cells gated on viable lymphocytes. FSC-H, Forward-scatter-height. (B) Fold change in ZAP-70 geometric MFI from baseline (0 s) at indicated times in CD8<sup>+</sup> and CD4<sup>+</sup> T cells for ED (blue lines,  $n = 17$ ) and AD (red lines,  $n = 4$ ) donors and (C) within CD8<sup>+</sup> and CD4<sup>+</sup> T cell differentiation subsets based on CD45RA and CD27 expression. Of note, ZAP-70 measurement was not included for the effector (CD45RA<sup>+</sup>CD27<sup>-</sup>) CD4<sup>+</sup> T cell population, as this subset was minimally expressed in CD4<sup>+</sup> T cells. (D) IFN- $\gamma$  and TNF cytokine expression in CD8<sup>+</sup> and CD4<sup>+</sup> T cells after stimulation of younger adults (red,  $n = 7$ ) and elderly adult (blue,  $n = 7$ ) PBMCs for 6 h ex vivo with PMA and ionomycin. Error bars represent SEM. Rectangles represent the second and third quartiles separated by the median horizontal line. Lower and upper quartiles are shown as vertical lines on either side of the rectangle. y/o, Years old

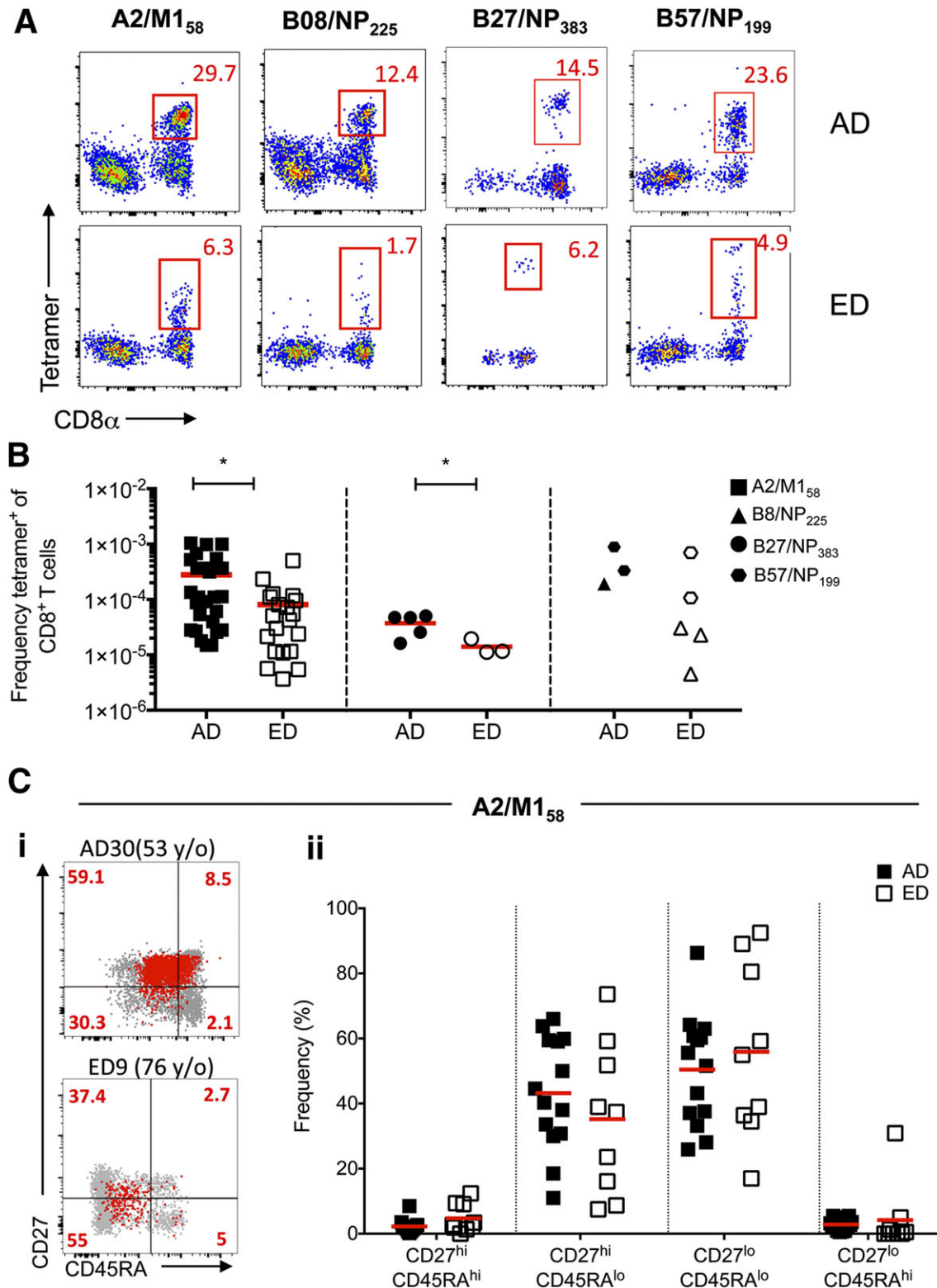


**FIGURE 3** Lower frequencies of elderly influenza-specific CD8<sup>+</sup> T cells across universal influenza HLAs. PBMCs from EDs and ADs were enriched for antigen-specific CD8<sup>+</sup> T cells using TAME. (A) Representative FACS plots of enriched fractions of epitope-specific CD8<sup>+</sup> T cells in ADs and EDs. Cells were gated as viable CD14<sup>−</sup>CD19<sup>−</sup>CD3<sup>+</sup>CD8<sup>+</sup>tetramer<sup>+</sup> cells. (B) Precursor frequencies of epitope-specific CD8<sup>+</sup> T cells of total CD8<sup>+</sup> T cells in ADs (closed symbols) and EDs (open symbols) for A2/M1<sub>58</sub>+CD8<sup>+</sup> T cells (AD:  $n = 27$ ; ED:  $n = 20$ ), B27/NP<sub>383</sub>+CD8<sup>+</sup> (AD:  $n = 5$ ; ED:  $n = 3$ ), and combined B8/NP<sub>225</sub>+CD8<sup>+</sup> (AD:  $n = 1$ ; ED:  $n = 3$ ) and B57/NP<sub>199</sub>+CD8<sup>+</sup> (AD:  $n = 2$ ; ED:  $n = 2$ ) frequencies (as a result of a limited number of donors), where  $1 \times 10^{-4}$  represents a frequency of 1 in 10,000 CD8<sup>+</sup> T cells. Mean and  $P$ -value symbols ( $*P < 0.05$ ; Student's  $t$  test) are shown. (Ci) Representative FACS plots of CD27 and CD45RA profiling of TAME-enriched, A2/M1<sub>58</sub>-specific CD8<sup>+</sup> T cells (in red) superimposed onto total CD8<sup>+</sup> T cells (in gray) in ADs and EDs. (ii) CD45RA<sup>−</sup>CD27<sup>+/−</sup> memory profiles of TAME-enriched, A2/M1<sub>58</sub>-specific CD8<sup>+</sup> T cells in ADs and EDs are comparable

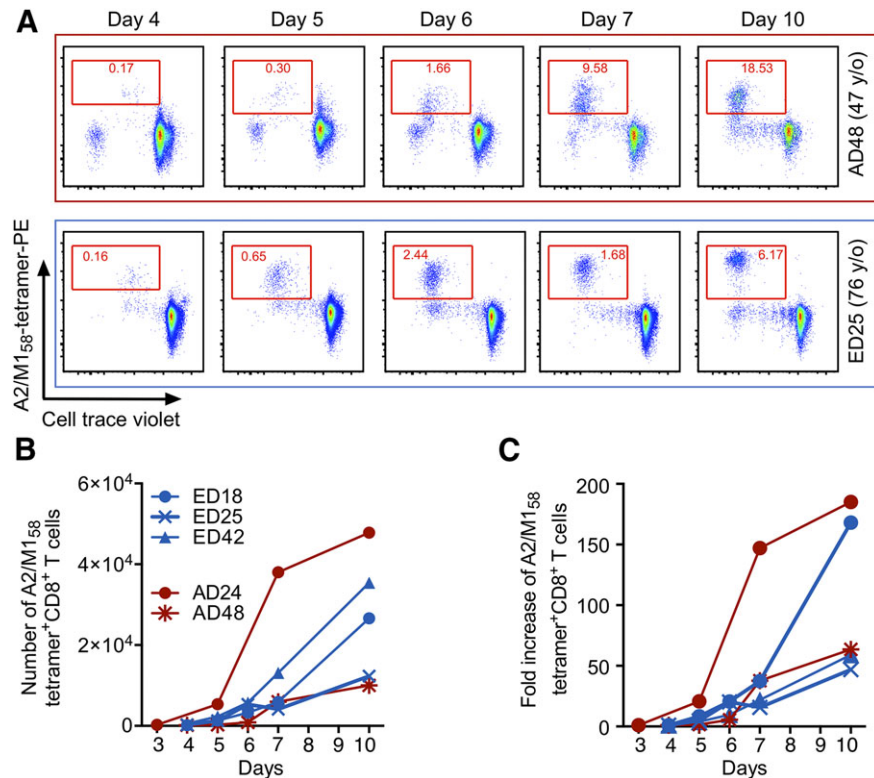


**FIGURE 4** In vitro proliferation of A2/M158-specific CD8<sup>+</sup> T cells. (A) Representative FACS plots of an AD (AD48) and ED (ED25) showing proliferation of expanded A2/M158-tetramer<sup>+</sup>CD8<sup>+</sup> T cells by the loss of cell trace violet over time. Cells were gated on total CD8<sup>+</sup> T cells and the values indicate percentages. (B) Total numbers and (C) fold increase of A2/M158-tetramer<sup>+</sup>CD8<sup>+</sup> T cells from the first detectable tetramer<sup>+</sup> time-point (d3 or -4), following in vitro expansion in ADs (red lines) and EDs (blue lines)

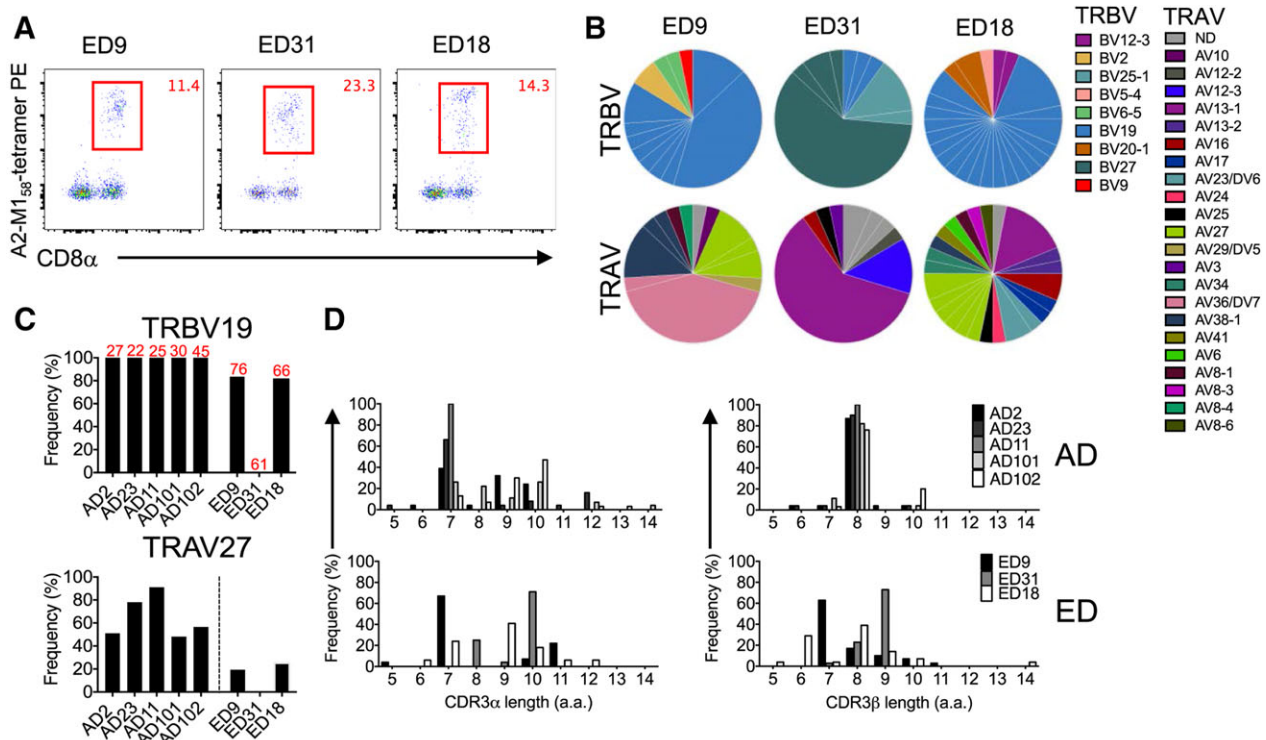


**FIGURE 5** Large expansions of private A2/M158<sup>+</sup>CD8<sup>+</sup> TCRαβ clonotypes in the elderly. Viable CD19<sup>−</sup>CD14<sup>−</sup>CD3<sup>+</sup>CD8<sup>+</sup>A2/M158-tetramer<sup>+</sup> T cells from 3 EDs were enriched by TAME and then single-cell sorted for TCRαβ analysis. (A) FACS plots of an enriched fraction of A2/M158-tetramer<sup>+</sup>CD8<sup>+</sup> T cells gated on CD3<sup>+</sup> T cells. Percentages in red are based on a gated CD8<sup>+</sup> T cell population. (B) Pie charts of TRBV and TRAV gene use. (C) Frequency of TRBV19 and TRAV27 gene use among ADs (numbers in red indicate age)<sup>35</sup> and EDs. (D) Distribution of CDR3α and CDR3β amino acid lengths in ADs and EDs. CDR3 lengths of ADs were taken from Valkenburg et al.<sup>35</sup>

Taken together, whereas the numbers of antigen-specific CD8<sup>+</sup> T cells across two universal HLAs are reduced in the elderly individuals, the activation/memory phenotype of those influenza-specific CD8<sup>+</sup> T cells remain stable.

### 3.4 | Robust proliferative capacity of A2/M1<sub>58</sub>-specific CD8<sup>+</sup> T cells in the elderly

Given that the numbers of influenza-specific CD8<sup>+</sup> T cells across several specificities were reduced in the elderly individuals, we next asked whether those epitope-specific CD8<sup>+</sup> T cells were capable of effective proliferation upon subsequent antigenic stimulation. We performed these experiments for the immunodominant influenza epitope, A2/M1<sub>58</sub>,<sup>35,46</sup> by *in vitro* A2/M1<sub>58</sub> peptide stimulation for 10 d. As *ex vivo* numbers of A2/M1<sub>58</sub> tetramer<sup>+</sup>CD8<sup>+</sup> T cells detected on d0 were below the detection limit, we used TAME to measure *ex vivo* d0 precursor frequencies (Fig. 3). Proliferation of A2/M1<sub>58</sub> tetramer<sup>+</sup>CD8<sup>+</sup> T cells was first observed between d3 and -4, as shown by the loss of cell trace violet over time (Fig. 4A). From undetectable levels on d0, the total numbers of A2/M1<sub>58</sub>-tetramer<sup>+</sup>CD8<sup>+</sup> T cells expanded similarly to  $1.0\text{--}4.8 \times 10^4$  cells in younger adults and  $1.2\text{--}3.5 \times 10^4$  cells in the elderly adults by d10 (Fig. 4B). Furthermore, fold expansions of A2/M1<sub>58</sub>-tetramer<sup>+</sup>CD8<sup>+</sup> T cells from d3 to d4 did not differ between elderly and younger adult cultures (Fig. 4C). Although our sample size was limited for these experiments, both younger and elderly adults had similar trends in the proliferation of A2/M1<sub>58</sub>-tetramer<sup>+</sup>CD8<sup>+</sup> T cells during the 10 d *in vitro* culture, as reflected in their fold increase of A2/M1<sub>58</sub>-tetramer<sup>+</sup>CD8<sup>+</sup> T cells at d7 and d10.

Given that our data suggest similar intrinsic TCR signaling capacity and expansion potential but reduced numbers of epitope-specific CD8<sup>+</sup> T cells in the elderly, we next asked whether such reduced numbers during aging were associated with striking alterations in the TCR $\alpha\beta$  repertoires of influenza-specific CD8<sup>+</sup> T cells.

### 3.5 | Large, noncanonical expansions of A2/M1<sub>58</sub>+CD8<sup>+</sup> TCR $\alpha\beta$ clonotypes in the elderly

To dissect the composition and diversity of epitope-specific TCR $\alpha\beta$  repertoires in the elderly, we used a single-cell multiplex RT-PCR capable of amplifying both TCR $\alpha$  and TCR $\beta$  chains.<sup>34,35,37,38</sup> Here, we provide the first *ex vivo* data on the paired epitope-specific TCR $\alpha\beta$  repertoire in the elderly. With the use of direct *ex vivo* tetramer staining, we examined TCR $\alpha\beta$  clonotypes within A2/M1<sub>58</sub>+CD8<sup>+</sup> T cells for 3 HLA-A\*02:01-expressing EDs (ED9, ED31, and ED18; Fig. 5A). As compared with our *ex vivo* TCR $\alpha\beta$  data for memory CD8<sup>+</sup> T cells in 5 young adults,<sup>35</sup> we found that the TCR $\alpha\beta$  repertoire in the EDs used a broader array of TRBV and TRAV gene use ( $n = 3.6$  and  $9.3$ , respectively) than in younger adults<sup>35</sup> ( $n = 1$  and  $5$ , respectively; Fig. 5B and Table 3). This suggests that the strong bias toward prominent TRAV27 and TRBV19 segments (as found in adults) decreases with aging and is replaced by a broader representation of TRAV and TRBV segments. The frequency of TRBV19 in the elderly was

decreased to a mean of 54.9% (range 0.0–83.5%), detected in 2/3 EDs, and was completely absent in another (ED31; Fig. 5C) compared with 100% TRBV19 gene use reported in 5 ADs (Fig. 5C). The prominence of TRAV27 was even more strikingly diminished, with a mean of 14.8% in the elderly (range of 0.0–25.1%) compared with younger adults, with a mean of 64.9% (range of 48.1–91.0%; Fig. 5C). Likewise, we observed marked differences in the use of complementarity-determining region  $\beta$  and  $\alpha$  (CDR3 $\beta$  and CDR3 $\alpha$ ; Fig. 5D). Whereas in younger adults the predominant CDR3 $\beta$  length is 8 aa [used by  $87 \pm 9\%$  (mean  $\pm$  SD) clonotypes], and CDR3 $\alpha$  length is 7 aa (used by  $48.8 \pm 34.7\%$  clonotypes),<sup>35</sup> these preferred CDR3 length features were reduced with aging (to  $26.3 \pm 11.4\%$  for CDR3 $\beta$  length and  $25.5 \pm 29.4\%$  for CDR3 $\alpha$ ), and instead, a broad range of both CDR3 $\beta$  and CDR3 $\alpha$  lengths was used in the EDs, and these varied greatly across different individuals (Fig. 5D).

Further dissection of CDR3 $\alpha\beta$  clonotypic signatures revealed that the elderly A2/M1<sub>58</sub>+CD8<sup>+</sup> T cells had a diminished sharing of the public TCR $\alpha\beta$  clonotype CDR3 $\beta$ -SIRSSYEQ (within TRBV19) and CDR3 $\alpha$ -GGSGQGNL (within TRAV27) and were found in only one ED (ED18) at 6.3% of the total TCR $\alpha\beta$  repertoire (Clone Y; Fig. 6A and Tables 3 and 4). Likewise, the well-documented CDR3 $\beta$  "IRS" amino acid sequence motif that provides a structural basis for peg-notch recognition of A2/M1<sub>58</sub><sup>47</sup> was present in both ADs and EDs (11/35 and 8/42 CDR3 $\beta$  clonotypes, respectively) but occurred less frequently, albeit not significantly, in the elderly ( $13.7 \pm 14.1\%$  of CDR3 $\beta$  sequences in elderly vs.  $32.4 \pm 29.6\%$  of CDR3 $\beta$ s in younger adults<sup>35</sup>). Thus, whereas public TCR $\beta$  signatures were still present, aging was associated with increased TCR $\beta$  diversity and oligoclonal expansion of clonotypes with longer CDR3 $\alpha$  loops. Conversely, the TCR $\alpha\beta$  repertoire in the elderly displayed more private clonotypes that were not typically shared across the EDs, except for clonotype (Clone C) bearing the public TCR $\beta$  sequence but a varied TCR $\alpha$  sequence, which was present in two EDs (Fig. 6B and Table 4). Interestingly, this was associated with large clonal expansions found in all of the elderly individuals, and these were characterized by longer CDR3 $\alpha$  loops (Table 4). This is most evident from ED31, characterized by 1 prominent TRAV13-1-TRBV27 TCR $\alpha\beta$  clonotype (Clone N), with a 10 aa CDR3 $\alpha$  constituting 60% of the A2/M1<sub>58</sub>+CD8<sup>+</sup> TCR $\alpha\beta$  repertoire (Fig. 6B and Table 4). In ED9, a large clonal expansion of a TRAV38-1-TRBV19 TCR $\alpha\beta$  clonotype with an 11 aa CDR3 $\alpha$  loop (Clone B; Table 4) was observed, further demonstrating that longer TCR $\alpha$  chain sequences can be detected in the EDs, in accordance with Gil et al.<sup>25</sup>

Overall, the influenza-specific A2/M1<sub>58</sub>+TCR $\alpha\beta$  repertoire in the elderly individuals varied strikingly from A2/M1<sub>58</sub>+TCR $\alpha\beta$  clonotypes observed in the ADs, with the main features being a reduction in the use of the public TRAV27-TRBV19 TCR $\alpha\beta$  clonotype, higher proportion of nonshared private TCR $\alpha\beta$  signatures, broader use of TRAV and TRBV segments, as well as large clonal expansion of selected private TCR $\alpha\beta$  clonotypes with longer CDR3 loops. Thus, it appears that with aging, changes within epitope-specific TCR $\alpha\beta$  repertoires are associated with selective loss of the public TCR $\alpha\beta$  and/or random clonal expansion of certain private TCRs.



**TABLE 3** Paired TRBV-TRBJ/TRAJ-TRAJ clonotype frequencies in ED

Clone ID	TRBV	TRBJ	CDR3b	Length	TRAV	TRAJ	CDR3a	Length	ED9	ED31	ED18
A	19	1-2	<b>SIGVAGY</b>	7	36/DV7	49	EDGTGNQ	7	41.6		
B	19	1-2	<b>SIGVAGY</b>	7	38-1	52	KDAGGTSYGKL	11	12.9		
C	19	2-7	<b>SIRSSYEQ</b>	8	27	42	AGSQGNL	7	9.7		6.3
D	2	1-1	<b>SEAPGLTNTTE</b>	10	27	38	ND		6.5		
E	6-5	1-2	SYLGVDGY	8	8-4	49	NTGNQ	5	3.2		
F	19	2-7	SIRSAYEQ	8	27	37	WLGSSTAGKL	10	3.2		
G	9	2-3	SVEGGGLTDTQ	11	29/DV5	32	SQGGGATNKL	10	3.2		
H	6-5	2-7	ND		10	10	ND		3.2		
I	19	1-2	<b>SIGVAGY</b>	7	ND		ND		3.2		
J	19	1-2	<b>SIGVAGY</b>	7	38-1	52	RGAGGTSYGKL	11	3.2		
K	19	1-2	SIVGTGYGY	9	8-1	45	GGGADGL	7	3.2		
L	19	1-2	<b>SIGVAGPTP</b>	9	38-1	52	KDAGGTSYGKL	11	3.2		
M	19	1-2	SIVGTGYGY	9	36/DV7	32	GGATNKL	7	3.2		
N	27	2-4	<b>SPLAGWDIQ</b>	9	13-1	54	<b>SMIIQGAQKL</b>	10		60.0	
O	25-1	2-3	<b>ARDRDNTQ</b>	8	12-3	26	<b>SAGNYGQN</b>	8		13.4	
P	27	2-4	<b>SPLAGWDIQ</b>	9	ND		ND			6.6	
Q	27	2-1	RTLDSYNE	8	3	9	RDKGGGKT	8		3.3	
R	27	2-7	SGQGLEQ	7	ND		ND			3.3	
S	19	2-3	SRGSTDQ	8	16	9	SEGRRHCNP	9		3.3	
T	19	2-1	SIGGVSYNE	9	25	27	LEANAGKS	8		3.3	
U	25-1	2-3	<b>ARDRDNTQ</b>	8	ND		ND			3.3	
V	19	2-7	SIGTTAEQ	8	12-2	42	KEGSQGNL	8		3.3	
W	19	2-3	<b>SSTDQ</b>	6	25	42	<b>NYGGSQGNL</b>	9			15.6
X	20-1	1-1	ND		41	58	<b>GEEETSGSRL</b>	10			6.3
Y	<u>19</u>	<u>2-7</u>	<u>SIRSSYEQ</u>	<u>8</u>	<u>27</u>	<u>42</u>	<u>GGSQGNL</u>	<u>7</u>			<u>6.3</u>
Z	19	2-1	SIGPGE	6	6	12	ND				3.1
AA	5-4	2-3	SDGTSGRGDGTDTQ	14	13-1	33	SLSGYQLI	8			3.1
AB	20-1	1-5	ND		16	29	ND				3.1
AC	19	2-3	SSRSTDQ	8	ND		ND				3.1
AD	19	1-5	SGRSNQPQ	8	13-2	53	ND				3.1
AE	19	1-6	ND		23/DV6	48	SMREGNEKL	9			3.1
AF	19	1-2	SGGGY	5	17	42	ND				3.1
AG	19	2-1	SPLAGGHNE	9	24	49	QTSNQ	6			3.1
AH	19	2-7	<b>SIRSSYEQ</b>	8	27	42	GGSQRNL	7			3.1
AI	19	1-2	SAGSYGY	7	38-1	52	TNAGGTSYGKL	11			3.1
AJ	19	2-7	SIRSAYEQ	8	8-6	42	SGSQGNL	7			3.1
AK	19	2-7	SSSYEQ	8	27	42	SAGGSQGNL	9			3.1
AL	19	2-1	SMSSGSYNE	9	8-1	20	ND				3.1
AM	19	2-7	SIRSAYEQ	8	27	37	GRTSKAGKL	9			3.1
AN	19	2-7	AIRSSYEQ	8	17	24	DWTDSWGKL	9			3.1
AO	12-3	2-2	SPLLAGGTGE	10	34	37	ASV#GSSNTGKL	12			3.1
AP	19	2-7	SSSYEQ	8	8-3	30	ND				3.1
AQ	19	2-7	<b>SIRSSYEQ</b>	8	27	37	AIGSSNTGKL	10			3.1
AR	19	1-5	SIHAGNQPQ	9	23/DV6	7	ND				3.1
AS	19	2-1	SIAGTTYNE	9	13-2	52	NTGANAGGTSYGKL	14			3.1
AT	12-3	2-2	SPLLAGGTGE	10	34	37	DQCGALATQGKL	12			3.1
Number of $\alpha\beta$ pairs									31	30	32

Clonotypes in bold represent the dominant clonotypes observed for each ED donor. Clonotype underlined (clone Y) represent the public A2/M1<sub>58</sub><sup>+</sup>TCR $\alpha\beta$  clonotype. Long CDR3 $\alpha$  a.a. lengths in italic are not commonly detected in younger adult donors.<sup>35</sup> ND, not determined.



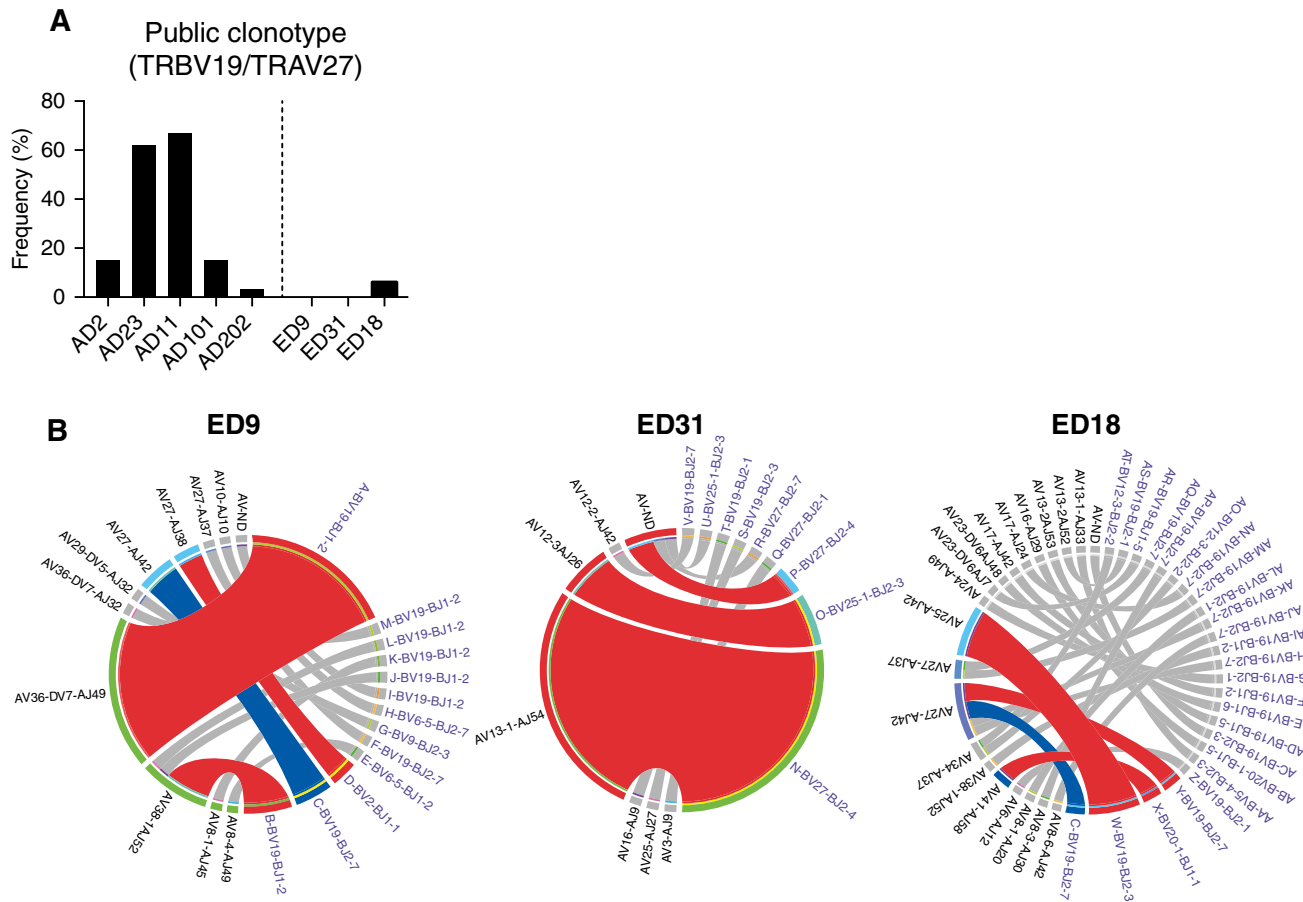


**FIGURE 6** Dominant private TCR $\alpha\beta$  clonotypes abundant in elderly. (A) Frequency of the public A2/M1<sub>58</sub><sup>+</sup>TCR $\alpha\beta$  clonotype is predominantly observed in ADs<sup>35</sup> but not EDs. (B) Circos plots of paired TRAV-TRAJ ( $\alpha\alpha$ ; black labels) and TRBV-TRBJ ( $\beta\beta$ ; blue labels) TCR clonotype analysis for each ED. Band width is proportional to the frequency, and each band represents a single clonotype. Red bands represent dominant private A2/M1<sub>58</sub><sup>+</sup>TCR $\alpha\beta$  clones from Table 4. Blue bands represent a shared TCR clone between ED9 and ED18 (Clone C). Gray bands represent other remaining clonotypes listed in Table 3

**TABLE 4** Paired TRBV-TRBJ/TRAJ-TRAJ frequencies of dominant TCR $\alpha\beta$  clones observed for each ED donor

Clone ID	TRBV	TRBJ	CDR3b	Length	TRAV	TRAJ	CDR3 $\alpha$	Length	ED9	ED31	ED18
A	19	1-2	SIGVAGY	7	36/DV7	49	EDGTGNQ	7	41.6		
B	19	1-2	SIGVAGY	7	38-1	52	KDAGGTSYGKL	11	12.9		
C	19	2-7	SIRSSYEQ	8	27	42	AGSQGNL	7	9.7		6.3
D	2	1-1	SEAPGLTNT	10	27	38	ND		6.5		
N	27	2-4	SPLAGWDIQ	9	13-1	54	SMIIQGAQKL	10		60.0	
O	25-1	2-3	ARDRDNTQ	8	12-3	26	SAGNYGQN	8		13.4	
P	27	2-4	SPLAGWDIQ	9	ND		ND			6.6	
W	19	2-3	SSTDTQ	6	25	42	NYGGSQGNL	9			15.6
X	20-1	1-1	ND		41	58	GEEETSGSRL	10			6.3
Y	19	2-7	SIRSSYEQ	8	27	42	GGSQGNL	7			6.3

Bold represents the public A2/M1<sub>58</sub><sup>+</sup> TCR $\alpha\beta$  clonotype.

## 4 | DISCUSSION

In the absence of neutralizing antibodies, one way of minimizing the effects of a novel influenza virus is to recall pre-existing, cross-strain, protective CD8<sup>+</sup> T cell memory directed at peptides derived from internal proteins shared by many influenza strains. Influenza-specific

CD8<sup>+</sup> T cells generated by seasonal influenza infection can promote virus elimination and host recovery, leading to a milder disease after infection with distinct strains.<sup>2,8-10,48</sup> Following the 2013 H7N9 avian influenza outbreak in China, we analyzed immune responses in patients hospitalized with severe and fatal influenza disease at the Shanghai Public Health Clinical Centre and found that recovery from

severe H7N9 disease was associated with diverse response mechanisms, driven predominantly by CD8<sup>+</sup> T cells.<sup>2</sup> We also provided evidence that the emergence of different effector mechanisms contributed to H7N9 disease resolution and survival. Patients with the most rapid recovery had early, robust, H7N9-specific CD8<sup>+</sup> T cell immunity, whereas those with prolonged hospital stays displayed late recruitment of CD8<sup>+</sup> and CD4<sup>+</sup> T cells and antibodies, augmented by NK cells. In contrast, individuals who died from severe H7N9 disease had no detectable influenza-specific immunity and no T cell activation, thus illustrating the importance of pre-existing CD8<sup>+</sup> T cell memory for protection against severe influenza disease (and death) caused by novel influenza viruses. However, it is far from clear what determines optimal, long-lasting, influenza-specific CD8<sup>+</sup> T cell immunity in humans and how such robust memory CD8<sup>+</sup> T cell responses persist throughout the human lifespan, which is particularly important, given our aging population and the fact that human lifespans are increasing. This reflects the relative paucity of data on human influenza-specific CD8<sup>+</sup> T cells, especially on the numbers of influenza-specific CD8<sup>+</sup> T cells and the underlying TCR $\alpha\beta$  characteristics, despite the great body of knowledge available for mice.

Here, we dissected ex vivo influenza-specific CD8<sup>+</sup> T cell responses and TCR $\alpha\beta$  clonal composition in elderly individuals and compared them with ADs. Our analyses showed that whereas bulk T cell compartments display increased frequencies of effector/memory T cells and altered transcription factor levels, we observed stable phenotype of influenza-specific CD8<sup>+</sup> T cells across different ages. Nevertheless, the numbers of influenza-specific CD8<sup>+</sup> T cells are reduced in the elderly, and they are characterized by large, noncanonical clonal expansions and reduced use of preferred TCR $\alpha\beta$  signatures (such as TRBV19 and TRAV27) and the public TRBV19–TRAV27 clonotype. Our findings suggest a need for new vaccination strategies to maintain the numbers and optimal TCR $\alpha\beta$  features of influenza-specific CD8<sup>+</sup> T cell immunity in elderly individuals.

Enhanced susceptibility to influenza and exacerbated disease severity can reflect overactivation of the innate immune system (cytokine storm, alveolar edema, and pulmonary complications) and impaired humoral and cellular immunity<sup>49</sup> and can be influenced by host genetic factors, such as HLA<sup>50</sup> or IFN-induced transmembrane protein 3.<sup>5</sup> The understanding of the key deficits that contribute to severe disease in high-risk groups is needed for the understanding of how immune interventions might minimize the incidence of severe influenza acute pneumonia. Our study provides new insights into how dysregulated CD8<sup>+</sup> T cell immunity, declining influenza-specific CD8<sup>+</sup> T cell numbers and perturbed TCR $\alpha\beta$  repertoires, may contribute to the higher infection rates and more severe disease observed for the elderly.

With the use of a human-adapted tetramer enrichment technique, naive, antigen-specific T cell precursor frequencies for HLA-A\*02:01-restricted NY-ESO-1<sub>1157–165</sub>, HIV Gag p1<sub>777–85</sub>, HCV Core<sub>132–140</sub>, CMV pp65<sub>495–503</sub>,<sup>45</sup> and WT1<sup>30</sup> antigens, in cancer-free and seronegative individuals, range between  $0.5 \times 10^{-6}$  and  $5.0 \times 10^{-6}$ . In comparison, frequencies of epitope-specific memory CD8<sup>+</sup> T cells are ~100 times higher, in the range of  $1$  in  $10^{-3}$ – $10^{-4}$  cells.<sup>30,35,45</sup> In our study, this was also the case for influenza-specific memory

CD8<sup>+</sup> T cells directed at the universal influenza epitopes in adults (pooled mean  $2.6 \times 10^{-4}$ ; range  $1.5 \times 10^{-5}$ – $1.0 \times 10^{-3}$ ) but reduced, on average, by 2.8-fold in elderly individuals (pooled mean  $9.2 \times 10^{-5}$ ; range  $3.7 \times 10^{-6}$ – $7.0 \times 10^{-4}$ ). Although the population coverage by the universal influenza HLAs varies greatly across different ethnicities (16–57%),<sup>26</sup> the maintenance of robust memory CD8<sup>+</sup> T cell pools directed at conserved viral regions is of importance for providing broad, long-lasting protection across different influenza strains, especially for the aging population at high risk from severe influenza disease. Our previous studies in mice show the following: 1) early priming of influenza-specific CD8<sup>+</sup> T cells preserves both the magnitude and TCR repertoire composition for the life of the experimental mouse,<sup>24</sup> and 2) sequential priming of the CD8<sup>+</sup> T cell compartment in the absence of antibody responses greatly reduces influenza-induced morbidity.<sup>51</sup> However, it is still unknown how frequently influenza-specific CD8<sup>+</sup> T cells in humans need to be primed to preserve the memory numbers and the optimal TCR repertoires. Recent evidence,<sup>29</sup> however, suggests that memory CD8<sup>+</sup> T cells are maintained in healthy donors for up to 12 yr. Furthermore, it is thought that humans are exposed to influenza viruses every 5–10 yr,<sup>52</sup> where natural infection would prime/boost T cell compartments. However, this would differ in vaccinated individuals, in whom neutralizing antibodies might prevent regular T cell boosting. However, despite the existing evidence in mice, there are still not enough data to understand how influenza-specific CD8<sup>+</sup> T cell immunity is generated and maintained in children. We still do not know how many times T cells need to be boosted in children for the maintenance of CD8<sup>+</sup> T cell numbers, effector function, and an optimal TCR repertoire. These are important questions for future studies.

The diversity and composition of the peripheral TCR $\alpha\beta$  repertoire have important implications for subsequent immune responses in both animal models and human disease.<sup>53</sup> Links among TCR repertoire diversity, public TCR usage, avidity, immune protection, and viral escape are well established.<sup>53–56</sup> In mice, the diverse and high peptide/MHC-I avidity of the D<sup>b</sup>PA<sub>224</sub>-specific TCR repertoire “protects” against viral escape during influenza infection. Conversely, emergence of escape variants occurs within the immunodominant D<sup>b</sup>NP<sub>366</sub> epitope, recognized by CD8<sup>+</sup> T cells expressing a restricted TCR $\beta$  repertoire.<sup>58</sup> The selection of CD8<sup>+</sup> T cell escape mutants is driven by selective pressure from D<sup>b</sup>NP<sub>366</sub>+CD8<sup>+</sup> T cells, as the NP<sub>366</sub> variants revert to the wild-type NP<sub>366</sub> sequence in the absence of immune pressure in MHC-mismatched mice.<sup>57</sup> Pre-emptive priming against the influenza viral mutants, however, can expand T cells expressing additional distinct TCRs that are capable of mounting robust recall responses against the viral variants.<sup>57</sup> Published evidence also points to the importance of TCR selection for viral control and disease-associated morbidity in human HIV, HCV, CMV, and influenza.<sup>57,59,60</sup> Although HCMV seropositivity can be one of the factors affecting immunosenescence and T cell responses to coinfecting viruses,<sup>61,62</sup> the HCMV status of our donors is unknown. It is most likely, as a diverse TCR repertoire provides a greater range of clonotypes with scope for the preferential selection of high-avidity TCRs into the immune response. This is particularly advantageous for disease control when diverse TCR repertoires with high peptide/MHC-I

avidity TCR clonotypes are capable of promoting superior CD8<sup>+</sup> T cell function and recognizing escape mutants.

In the current study, we provide the first ex vivo data on paired epitope-specific TCR $\alpha\beta$  clonotypes in the elderly, showing that the influenza-specific A2/M1<sub>58</sub><sup>+</sup>TCR $\alpha\beta$  repertoires in the EDs vary from that in younger adults, with the main features being a reduction in the frequency of the public TRBV19–TRAV27 TCR $\alpha\beta$  clonotype; an increased proportion of nonshared, private TCR $\alpha\beta$  signatures; broader use of TRAV and TRBV segments; and large clonal expansion of private TCR $\alpha\beta$  clonotypes with longer CDR3 $\alpha$  loops. These are striking alterations within the A2/M1<sub>58</sub> TCR $\alpha\beta$  repertoire, especially with respect to the lack of the prominent, public TCR $\alpha\beta$  clonotype, which has previously been shown to have a characteristic peg-and-notch mode of A2/M1<sub>58</sub> peptide recognition<sup>47</sup> and is capable of recognizing both the wild-type peptide as well as the mutated versions of the A2/M1<sub>58</sub> peptide found in circulating influenza viruses.<sup>35</sup> It is possible that with aging, there may be a shift or skewing in the predominant structural basis of A2/M1<sub>58</sub> recognition by the TCR $\alpha\beta$  repertoire, which may have implications for the protective capacity of the A2/M1<sub>58</sub>-specific CD8<sup>+</sup> T cell response. Selection of public clones (exactly the same TCRs shared among unrelated individuals) is also associated with superior CD8<sup>+</sup> T cell immunity during HIV-1 infection, whereas a lack of the public clonotypes leads to suboptimal immunity.<sup>59</sup> Thus, large, random clonal expansions, rather than preservation of the key public TCR $\alpha\beta$  clonotypes, appear to be features of the aging TCR $\alpha\beta$  repertoire, in accordance with previous studies in mice and humans.<sup>25,63</sup>

One caveat of our study was our inability to assess directly the TCR signaling capacity of epitope-specific CD8<sup>+</sup> T cells in the younger adults compared with EDs. As a result of the low frequencies of tetramer-specific CD8<sup>+</sup> T cells in 100  $\mu$ l blood, our ex vivo ZAP-70 signaling assay could not be modified to determine TCR-mediated ZAP-70 phosphorylation efficacy in influenza-specific CD8<sup>+</sup> T cells. Although based on our previous studies in mice,<sup>64,65</sup> we speculate that the M1<sub>58</sub>-specific TCR repertoires lacking the “best-fit,” immunodominant, public clonotypes in EDs, might have less of an effector function compared with younger adult M1<sub>58</sub>-specific TCR repertoires, predominantly encompassing the public clonotypes.

The future design of T cell-based vaccination strategies should provide effective, long-lasting protection across the lifespan of an individual. The changes to the composition and protective abilities of T cell memory subsets across the human lifespan require future studies to understand what constitutes optimal T cell memory. The potential complicating factors in the maintenance of life-long immunity are the changes at the cellular and molecular levels, which occur during aging and have been associated with impaired immune responsiveness in the elderly. However, studies, to date, suggest that age-related defects in T cell immunity predominantly affect the generation and maintenance of T cell memory in old age. This indicates that the counteracting of increased immune susceptibility in the elderly may require either the development of vaccines to be administered early in life to generate long-lasting T cell memory, even for pathogens likely to be encountered later in life, or the development of strategies to prevent age-related perturbations in T cell immunity. Either approach might

potentially boost antigen-specific CD8<sup>+</sup> T cell numbers and maintain optimal TCR $\alpha\beta$  repertoires for life.

## AUTHORSHIP

T.H.O.N. and S.S. are joint first authors. L.L. and K.K. share senior authorship. T.H.O.N., S.S., S.G., J.C., L.L., and K.K. designed research. T.H.O.N., S.S., N.L.B., E.J.G., E.B.C., M.K., S.G., and L.L. performed research. T.H.O.N., S.S., N.L.B., S.A.V., L.L., and K.K. analyzed data. A.J. provided the ZAP-70 assay and expertise. M.L. and J.C. provided crucial donor samples. T.H.O.N., S.S., L.L., and K.K. wrote the paper. All authors read and edited the manuscript.

## ACKNOWLEDGMENTS

S.S. is a recipient of the Victoria India Doctoral Scholarship and Melbourne International Fee Remission Scholarship (MIFRS), University of Melbourne. E.J.G. is an Australian National Health and Medical Research Council (NHMRC) CJ Martin Fellow. E.B.C. is an NHMRC Peter Doherty Fellow. M.K. is supported by a Melbourne International Research Scholarship (MIRS) and MIFRS. M.L. is supported by an NHMRC Career Development Fellowship (ID 1047025). K.K. is supported by an NHMRC program grant (ID 1071916) and the NHMRC Senior Research Fellowship Level B. The authors thank Thakshila Amarasena and Sheilajen Alcantara for their technical assistance. The authors also thank all donors for donating blood for this study and Bernie McCudden for collecting blood. The authors thank the clinical research midwives, Genevieve Christophers, Gabrielle Pell, and Rachel Murdoch, for the CB sample collection and the Obstetrics and Midwifery staff of Mercy Hospital for Women for their cooperation. The authors thank Matthew Caverley and Paul Thomas for their technical expertise in TCR sequence analysis.

## DISCLOSURES

The authors declare no conflicts of interest.

## REFERENCES

1. Kucharski, A. J., Lessler, J., Read, J. M., Zhu, H., Jiang, C. Q., Guan, Y., Cummings, D. A., Riley, S. (2015) Estimating the life course of influenza A(H3N2) antibody responses from cross-sectional data. *PLoS Biol.* 13, e1002082.
2. Wang, Z., Wan, Y., Qiu, C., Quiñones-Parra, S., Zhu, Z., Loh, L., Tian, D., Ren, Y., Hu, Y., Zhang, X., Thomas, P. G., Inouye, M., Doherty, P. C., Kedzierska, K., Xu, J. (2015) Recovery from severe H7N9 disease is associated with diverse response mechanisms dominated by CD8<sup>+</sup> T cells. *Nat. Commun.* 6, 6833.
3. Cheng, A. C., Holmes, M., Dwyer, D. E., Irving, L. B., Korman, T. M., Senenayake, S., Macartney, K. K., Blyth, C. C., Brown, S., Waterer, G., Hwer, R., Friedman, N. D., Wark, P. A., Simpson, G., Upham, J., Bowler, S. D., Lessing, A., Kotsimbos, T., Kelly, P. M. (2016) Influenza epidemiology in patients admitted to sentinel Australian hospitals in 2015: the Influenza Complications Alert Network. *Commun. Dis. Intell. Q. Rep.* 40, E521–E526.
4. Fiore, A. E., Uyeki, T. M., Broder, K., Finelli, L., Euler, G. L., Singleton, J. A., Iskander, J. K., Wortley, P. M., Shay, D. K., Bresee, J. S., Cox, N. J.; Centers for Disease Control and Prevention (CDC). (2010) Prevention and control of influenza with vaccines: recommendations of the Advisory

- Committee on Immunization Practices (ACIP), 2010. *MMWR Recomm. Rep.* 59, 1–62.
5. Wang, Z., Zhang, A., Wan, Y., Liu, X., Qiu, C., Xi, X., Ren, Y., Wang, J., Dong, Y., Bao, M., Li, L., Zhou, M., Yuan, S., Sun, J., Zhu, Z., Chen, L., Li, Q., Zhang, Z., Zhang, X., Lu, S., Doherty, P. C., Kedzierska, K., Xu, J. (2014) Early hypercytokinemia is associated with interferon-induced transmembrane protein-3 dysfunction and predictive of fatal H7N9 infection. *Proc. Natl. Acad. Sci. USA* 111, 769–774.
  6. Gao, R., Cao, B., Hu, Y., Feng, Z., Wang, D., Hu, W., Chen, J., Jie, Z., Qiu, H., Xu, K., Xu, X., Lu, H., Zhu, W., Gao, Z., Xiang, N., Shen, Y., He, Z., Gu, Y., Zhang, Z., Yang, Y., Zhao, X., Zhou, L., Li, X., Zou, S., Zhang, Y., Li, X., Yang, L., Guo, J., Dong, J., Li, Q., Dong, L., Zhu, Y., Bai, T., Wang, S., Hao, P., Yang, W., Zhang, Y., Han, J., Yu, H., Li, D., Gao, G. F., Wu, G., Wang, Y., Yuan, Z., Shu, Y. (2013) Human infection with a novel avian-origin influenza A (H7N9) virus. *N. Engl. J. Med.* 368, 1888–1897.
  7. Goronzy, J. J., Weyand, C. M. (2017) Successful and maladaptive T cell aging. *Immunity* 46, 364–378.
  8. McMichael, A. J., Gotch, F. M., Noble, G. R., Beare, P. A. (1983) Cytotoxic T-cell immunity to influenza. *N. Engl. J. Med.* 309, 13–17.
  9. Hayward, A. C., Wang, L., Goonetilleke, N., Fragaszy, E. B., Bermingham, A., Copas, A., Dukes, O., Millett, E. R., Nazareth, I., Nguyen-Van-Tam, J. S., Watson, J. M., Zambon, M., Flu Watch Group, Johnson, A. M., McMichael, A. J. (2015) Natural T cell-mediated protection against seasonal and pandemic influenza. Results of the Flu Watch Cohort Study. *Am. J. Respir. Crit. Care Med.* 191, 1422–1431.
  10. Sridhar, S., Begom, S., Bermingham, A., Hoschler, K., Adamson, W., Carman, W., Bean, T., Barclay, W., Deeks, J. J., Lalvani, A. (2013) Cellular immune correlates of protection against symptomatic pandemic influenza. *Nat. Med.* 19, 1305–1312.
  11. Yunis, E. J., Fernandes, G., Smith, J., Stutman, O., Good, R. A. (1973) Involution of the thymus dependent lymphoid system. *Adv. Exp. Med. Biol.* 29, 301–306.
  12. Simpson, J. G., Gray, E. S., Beck, J. S. (1975) Age involution in the normal human adult thymus. *Clin. Exp. Immunol.* 19, 261–265.
  13. Vezys, V., Yates, A., Casey, K. A., Lanier, G., Ahmed, R., Antia, R., Masopust, D. (2009) Memory CD8 T-cell compartment grows in size with immunological experience. *Nature* 457, 196–199.
  14. Cicin-Sain, L., Messaoudi, I., Park, B., Currier, N., Planer, S., Fischer, M., Tackitt, S., Nikolich-Zugich, D., Legasse, A., Axthelm, M. K., Picker, L. J., Mori, M., Nikolich-Zugich, J. (2007) Dramatic increase in naive T cell turnover is linked to loss of naive T cells from old primates. *Proc. Natl. Acad. Sci. USA* 104, 19960–19965.
  15. Effros, R. B. (1996) Insights on immunological aging derived from the T lymphocyte cellular senescence model. *Exp. Gerontol.* 31, 21–27.
  16. Ouyang, Q., Wagner, W. M., Walter, S., Müller, C. A., Wikby, A., Aubert, G., Klatt, T., Stevanovic, S., Dodi, T., Pawelec, G. (2003) An age-related increase in the number of CD8+ T cells carrying receptors for an immunodominant Epstein-Barr virus (EBV) epitope is counteracted by a decreased frequency of their antigen-specific responsiveness. *Mech. Ageing Dev.* 124, 477–485.
  17. Ely, K. H., Ahmed, M., Kohlmeier, J. E., Roberts, A. D., Wittmer, S. T., Blackman, M. A., Woodland, D. L. (2007) Antigen-specific CD8+ T cell clonal expansions develop from memory T cell pools established by acute respiratory virus infections. *J. Immunol.* 179, 3535–3542.
  18. Kohlmeier, J. E., Connor, L. M., Roberts, A. D., Cookenham, T., Martin, K., Woodland, D. L. (2010) Nonmalignant clonal expansions of memory CD8+ T cells that arise with age vary in their capacity to mount recall responses to infection. *J. Immunol.* 185, 3456–3462.
  19. McElhaney, J. E., Gravenstein, S., Upshaw, C. M., Hooton, J. W., Krause, P., Drinka, P., Bleackley, R. C. (2001) Granzyme B: a marker of risk for influenza in institutionalized older adults. *Vaccine* 19, 3744–3751.
  20. Globerson, A., Effros, R. B. (2000) Ageing of lymphocytes and lymphocytes in the aged. *Immunol. Today* 21, 515–521.
  21. Ahmed, M., Lanzer, K. G., Yager, E. J., Adams, P. S., Johnson, L. L., Blackman, M. A. (2009) Clonal expansions and loss of receptor diversity in the naive CD8 T cell repertoire of aged mice. *J. Immunol.* 182, 784–792.
  22. Yager, E. J., Ahmed, M., Lanzer, K., Randall, T. D., Woodland, D. L., Blackman, M. A. (2008) Age-associated decline in T cell repertoire diversity leads to holes in the repertoire and impaired immunity to influenza virus. *J. Exp. Med.* 205, 711–723.
  23. Rudd, B. D., Venturi, V., Davenport, M. P., Nikolich-Zugich, J. (2011) Evolution of the antigen-specific CD8+ TCR repertoire across the life span: evidence for clonal homogenization of the old TCR repertoire. *J. Immunol.* 186, 2056–2064.
  24. Valkenburg, S. A., Venturi, V., Dang, T. H., Bird, N. L., Doherty, P. C., Turner, S. J., Davenport, M. P., Kedzierska, K. (2012) Early priming minimizes the age-related immune compromise of CD8+ T cell diversity and function. *PLoS Pathog.* 8, e1002544.
  25. Gil, A., Yassai, M. B., Naumov, Y. N., Selin, L. K. (2015) Narrowing of human influenza A virus-specific T cell receptor  $\alpha$  and  $\beta$  repertoires with increasing age. *J. Virol.* 89, 4102–4116.
  26. Quiñones-Parra, S., Grant, E., Loh, L., Nguyen, T. H., Campbell, K. A., Tong, S. Y., Miller, A., Doherty, P. C., Vijaykrishna, D., Rossjohn, J., Gras, S., Kedzierska, K. (2014) Preexisting CD8+ T-cell immunity to the H7N9 influenza A virus varies across ethnicities. *Proc. Natl. Acad. Sci. USA* 111, 1049–1054.
  27. Yu, H., Cowling, B. J., Feng, L., Lau, E. H., Liao, Q., Tsang, T. K., Peng, Z., Wu, P., Liu, F., Fang, V. J., Zhang, H., Li, M., Zeng, L., Xu, Z., Li, Z., Luo, H., Li, Q., Feng, Z., Cao, B., Yang, W., Wu, J. T., Wang, Y., Leung, G. M. (2013) Human infection with avian influenza A H7N9 virus: an assessment of clinical severity. *Lancet* 382, 138–145.
  28. Van de Sandt, C. E., Kreijtz, J. H., de Mutsert, G., Geelhoed-Mieras, M. M., Hillaire, M. L., Vogelzang-van Trierum, S. E., Osterhaus, A. D., Fouchier, R. A., Rimmelzwaan, G. F. (2014) Human cytotoxic T lymphocytes directed to seasonal influenza A viruses cross-react with the newly emerging H7N9 virus. *J. Virol.* 88, 1684–1693.
  29. Van de Sandt, C. E., Hillaire, M. L., Geelhoed-Mieras, M. M., Osterhaus, A. D., Fouchier, R. A., Rimmelzwaan, G. F. (2015) Human influenza A virus-specific CD8+ T-cell response is long-lived. *J. Infect. Dis.* 212, 81–85.
  30. Nguyen, T. H., Tan, A. C., Xiang, S. D., Goubier, A., Harland, K. L., Clemens, E. B., Plebanski, M., Kedzierska, K. (2017) Understanding CD8(+) T-cell responses toward the native and alternate HLA-A\*02:01-restricted WT1 epitope. *Clin. Transl. Immunology* 6, e134.
  31. Gras, S., Burrows, S. R., Kjer-Nielsen, L., Clements, C. S., Liu, Y. C., Sullivan, L. C., Bell, M. J., Brooks, A. G., Purcell, A. W., McCluskey, J., Rossjohn, J. (2009) The shaping of T cell receptor recognition by self-tolerance. *Immunity* 30, 193–203.
  32. Lichtfuss, G. F., Meehan, A. C., Cheng, W. J., Cameron, P. U., Lewin, S. R., Crowe, S. M., Jaworowski, A. (2011) HIV inhibits early signal transduction events triggered by CD16 cross-linking on NK cells, which are important for antibody-dependent cellular cytotoxicity. *J. Leukoc. Biol.* 89, 149–158.
  33. Nguyen, T. H., Bird, N. L., Grant, E. J., Miles, J. J., Thomas, P. G., Kotsimbos, T. C., Mifsud, N. A., Kedzierska, K. (2017) Maintenance of the EBV-specific CD8(+) TCR $\alpha\beta$  repertoire in immunosuppressed lung transplant recipients. *Immunol. Cell Biol.* 95, 77–86.
  34. Grant, E. J., Josephs, T. M., Valkenburg, S. A., Wooldridge, L., Hellard, M., Rossjohn, J., Bharadwaj, M., Kedzierska, K., Gras, S. (2016) Lack of heterologous cross-reactivity toward HLA-A\*02:01 restricted viral epitopes is underpinned by distinct  $\alpha\beta$  T cell receptor signatures. *J. Biol. Chem.* 291, 24335–24351.



35. Valkenburg, S. A., Josephs, T. M., Clemens, E. B., Grant, E. J., Nguyen, T. H., Wang, G. C., Price, D. A., Miller, A., Tong, S. Y., Thomas, P. G., Doherty, P. C., Rossjohn, J., Gras, S., Kedzierska, K. (2016) Molecular basis for universal HLA-A\*0201-restricted CD8+ T-cell immunity against influenza viruses. *Proc. Natl. Acad. Sci. USA* 113, 4440–4445.
36. Gras, S., Kedzierski, L., Valkenburg, S. A., Laurie, K., Liu, Y. C., Denholm, J. T., Richards, M. J., Rimmelzwaan, G. F., Kelso, A., Doherty, P. C., Turner, S. J., Rossjohn, J., Kedzierska, K. (2010) Cross-reactive CD8+ T-cell immunity between the pandemic H1N1-2009 and H1N1-1918 influenza A viruses. *Proc. Natl. Acad. Sci. USA* 107, 12599–12604.
37. Wang, G. C., Dash, P., McCullers, J. A., Doherty, P. C., Thomas, P. G. (2012) T cell receptor  $\alpha\beta$  diversity inversely correlates with pathogen-specific antibody levels in human cytomegalovirus infection. *Sci. Transl. Med.* 4, 128ra42.
38. Nguyen, T. H., Rowntree, L. C., Pellicci, D. G., Bird, N. L., Handel, A., Kjer-Nielsen, L., Kedzierska, K., Kotsimbos, T. C., Mifsud, N. A. (2014) Recognition of distinct cross-reactive virus-specific CD8+ T cells reveals a unique TCR signature in a clinical setting. *J. Immunol.* 192, 5039–5049.
39. Brochet, X., Lefranc, M. P., Giudicelli, V. (2008) IMGT/V-QUEST: the highly customized and integrated system for IG and TR standardized V-J and V-D-J sequence analysis. *Nucleic Acids Res.* 36, W503–W508.
40. Folch, G., Scaviner, D., Contet, V., Lefranc, M. P. (2000) Protein displays of the human T cell receptor alpha, beta, gamma and delta variable and joining regions. *Exp. Clin. Immunogenet.* 17, 205–215.
41. Krzywinski, M., Schein, J., Birol, I., Connors, J., Gascoyne, R., Horsman, D., Jones, S. J., Marra, M. A. (2009) Circos: an information aesthetic for comparative genomics. *Genome Res.* 19, 1639–1645.
42. Dolfi, D. V., Mansfield, K. D., Polley, A. M., Doyle, S. A., Freeman, G. J., Pircher, H., Schmadier, K. E., Wherry, E. J. (2013) Increased T-bet is associated with senescence of influenza virus-specific CD8 T cells in aged humans. *J. Leukoc. Biol.* 93, 825–836.
43. Geginat, J., Lanzavecchia, A., Sallusto, F. (2003) Proliferation and differentiation potential of human CD8+ memory T-cell subsets in response to antigen or homeostatic cytokines. *Blood* 101, 4260–4266.
44. Wherry, E. J., Kurachi, M. (2015) Molecular and cellular insights into T cell exhaustion. *Nat. Rev. Immunol.* 15, 486–499.
45. Alanio, C., Lemaitre, F., Law, H. K., Hasan, M., Albert, M. L. (2010) Enumeration of human antigen-specific naive CD8+ T cells reveals conserved precursor frequencies. *Blood* 115, 3718–3725.
46. Hillaire, M. L., van Trierum, S. E., Bodewes, R., van Baalen, C. A., van Binnendijk, R. S., Koopmans, M. P., Fouchier, R. A., Osterhaus, A. D., Rimmelzwaan, G. F. (2011) Characterization of the human CD8+ T cell response following infection with 2009 pandemic influenza H1N1 virus. *J. Virol.* 85, 12057–12061.
47. Stewart-Jones, G. B., McMichael, A. J., Bell, J. I., Stuart, D. I., Jones, E. Y. (2003) A structural basis for immunodominant human T cell receptor recognition. *Nat. Immunol.* 4, 657–663.
48. Kreijtz, J. H., de Mutsert, G., van Baalen, C. A., Fouchier, R. A., Osterhaus, A. D., Rimmelzwaan, G. F. (2008) Cross-recognition of avian H5N1 influenza virus by human cytotoxic T-lymphocyte populations directed to human influenza A virus. *J. Virol.* 82, 5161–5166.
49. La Gruta, N. L., Kedzierska, K., Stambas, J., Doherty, P. C. (2007) A question of self-preservation: immunopathology in influenza virus infection. *Immunol. Cell Biol.* 85, 85–92.
50. Hertz, T., Oshansky, C. M., Roddam, P. L., DeVincenzo, J. P., Caniza, M. A., Jojic, N., Mallal, S., Phillips, E., James, I., Halloran, M. E., Thomas, P. G., Corey, L. (2013) HLA targeting efficiency correlates with human T-cell response magnitude and with mortality from influenza A infection. *Proc. Natl. Acad. Sci. USA* 110, 13492–13497.
51. Quiñones-Parra, S. M., Clemens, E. B., Wang, Z., Croom, H. A., Kedzierski, L., McVernon, J., Vijaykrishna, D., Kedzierska, K. (2016) A role of influenza virus exposure history in determining pandemic susceptibility and CD8+ T cell responses. *J. Virol.* 90, 6936–6947.
52. Fonville, J. M., Wilks, S. H., James, S. L., Fox, A., Ventresca, M., Aban, M., Xue, L., Jones, T. C., Le, N. M. H., Pham, Q. T., Tran, N. D., Wong, Y., Mosterin, A., Katzelnick, L. C., Labonte, D., Le, T. T., van der Net, G., Skepner, E., Russell, C. A., Kaplan, T. D., Rimmelzwaan, G. F., Masurel, N., de Jong, J. C., Palache, A., Beyer, W. E. P., Le, Q. M., Nguyen, T. H., Wertheim, H. F. L., Hurt, A. C., Osterhaus, A. D. M. E., Barr, I. G., Fouchier, R. A. M., Horby, P. W., Smith, D. J. (2014) Antibody landscapes after influenza virus infection or vaccination. *Science* 346, 996–1000.
53. Miles, J. J., Douek, D. C., Price, D. A. (2011) Bias in the  $\alpha\beta$  T-cell repertoire: implications for disease pathogenesis and vaccination. *Immunol. Cell Biol.* 89, 375–387.
54. Messaoudi, I., Guevara Patiño, J. A., Dyal, R., LeMaout, J., Nikolich-Zugich, J. (2002) Direct link between mhc polymorphism, T cell avidity, and diversity in immune defense. *Science* 298, 1797–1800.
55. Price, D. A., Brenchley, J. M., Ruff, L. E., Betts, M. R., Hill, B. J., Roederer, M., Koup, R. A., Migueles, S. A., Gostick, E., Wooldridge, L., Sewell, A. K., Connors, M., Douek, D. C. (2005) Avidity for antigen shapes clonal dominance in CD8+ T cell populations specific for persistent DNA viruses. *J. Exp. Med.* 202, 1349–1361.
56. Price, D. A., West, S. M., Betts, M. R., Ruff, L. E., Brenchley, J. M., Ambrozak, D. R., Edghill-Smith, Y., Kuroda, M. J., Bogdan, D., Kunstman, K., Letvin, N. L., Franchini, G., Wolinsky, S. M., Koup, R. A., Douek, D. C. (2004) T cell receptor recognition motifs govern immune escape patterns in acute SIV infection. *Immunity* 21, 793–803.
57. Valkenburg, S. A., Quiñones-Parra, S., Gras, S., Komadina, N., McVernon, J., Wang, Z., Halim, H., Iannello, P., Cole, C., Laurie, K., Kelso, A., Rossjohn, J., Doherty, P. C., Turner, S. J., Kedzierska, K. (2013) Acute emergence and reversion of influenza A virus quasiespecies within CD8+ T cell antigenic peptides. *Nat. Commun.* 4, 2663.
58. Kedzierska, K., Turner, S. J., Doherty, P. C. (2004) Conserved T cell receptor usage in primary and recall responses to an immunodominant influenza virus nucleoprotein epitope. *Proc. Natl. Acad. Sci. USA* 101, 4942–4947.
59. Chen, H., Ndhlovu, Z. M., Liu, D., Porter, L. C., Fang, J. W., Darko, S., Brockman, M. A., Miura, T., Brumme, Z. L., Schneidewind, A., Piechocka-Trocha, A., Cesa, K. T., Sela, J., Cung, T. D., Toth, I., Pereyra, F., Yu, X. G., Douek, D. C., Kaufmann, D. E., Allen, T. M., Walker, B. D. (2012) TCR clonotypes modulate the protective effect of HLA class I molecules in HIV-1 infection. *Nat. Immunol.* 13, 691–700.
60. Ladell, K., Hashimoto, M., Iglesias, M. C., Wilmann, P. G., McLaren, J. E., Gras, S., Chikata, T., Kuse, N., Fastenackels, S., Gostick, E., Bridgeman, J. S., Venturi, V., Arkoub, Z. A., Agut, H., van Bockel, D. J., Almeida, J. R., Douek, D. C., Meyer, L., Venet, A., Takiguchi, M., Rossjohn, J., Price, D. A., Appay, V. (2013) A molecular basis for the control of preimmune escape variants by HIV-specific CD8+ T cells. *Immunity* 38, 425–436.
61. Solana, R., Tarazona, R., Aiello, A. E., Akbar, A. N., Appay, V., Beswick, M., Bosch, J. A., Campos, C., Cantisán, S., Cicin-Sain, L., Derhovanessian, E., Ferrando-Martínez, S., Frasca, D., Fulöp, T., Govind, S., Grubeck-Loebenstein, B., Hill, A., Hurme, M., Kern, F., Larbi, A., López-Botet, M., Maier, A. B., McElhaney, J. E., Moss, P., Naumova, E., Nikolich-Zugich, J., Pera, A., Rector, J. L., Riddell, N., Sanchez-Correa, B., Sansoni, P., Sauce, D., van Lier, R., Wang, G. C., Wills, M. R., Zieliński, M., Pawelec, G. (2012) CMV and Immunosenescence: from basics to clinics. *Immun. Ageing* 9, 23.
62. Furman, D., Jojic, V., Sharma, S., Shen-Orr, S. S., Angel, C. J., Onengut-Gumuscu, S., Kidd, B. A., Maecker, H. T., Concannon, P., Dekker, C. L., Thomas, P. G., Davis, M. M. (2015) Cytomegalovirus infection enhances the immune response to influenza. *Sci. Transl. Med.* 7, 281ra43.
63. Pulko, V., Davies, J. S., Martinez, C., Lanteri, M. C., Busch, M. P., Diamond, M. S., Knox, K., Bush, E. C., Sims, P. A., Sinari, S., Billheimer, D.,



- Haddad, E. K., Murray, K. O., Wertheimer, A. M., Nikolich-Zugich, J. (2016) Human memory T cells with a naive phenotype accumulate with aging and respond to persistent viruses. *Nat. Immunol.* 17, 966–975.
64. Turner, S. J., Kedzierska, K., Komodromou, H., La Gruta, N. L., Dunstone, M. A., Webb, A. I., Webby, R., Walden, H., Xie, W., McCluskey, J., Purcell, A. W., Rossjohn, J., Doherty, P. C. (2005) Lack of prominent peptide-major histocompatibility complex features limits repertoire diversity in virus-specific CD8<sup>+</sup> T cell populations. *Nat. Immunol.* 6, 382–389.
65. Valkenburg, S. A., Gras, S., Guillonneau, C., La Gruta, N. L., Thomas, P. G., Purcell, A. W., Rossjohn, J., Doherty, P. C., Turner, S. J., Kedzierska, K. (2010) Protective efficacy of cross-reactive CD8<sup>+</sup> T cells recognising mutant viral epitopes depends on peptide-MHC-I structural interactions and T cell activation threshold. *PLoS Pathog.* 6, e1001039.

**How to cite this article:** Nguyen THO, Sant S, Bird NL, et al. Perturbed CD8<sup>+</sup> T cell immunity across universal influenza epitopes in the elderly. *J Leukoc Biol.* 2018;103: 321–339. <https://doi.org/10.1189/jlb.5MA0517-207R>